2012

Quality Assessment of Geogrids Used for Subgrade Treatment

Min Sang Lee
Purdue University, lee195@purdue.edu

Yoon Seok Choi
Purdue University, choi59@purdue.edu

Monica Prezzi
Purdue University, mprezzi@purdue.edu

Recommended Citation
Lee, M., Y. Choi, and M. Prezzi. *Quality Assessment of Geogrids Used for Subgrade Treatment*. Publication FHWA/IN/JTRP-2012/27. Joint Transportation Research Program, Indiana Department of Transportation and Purdue University, West Lafayette, Indiana, 2012. doi: 10.5703/1288284315034.

JOINT TRANSPORTATION RESEARCH PROGRAM

INDIANA DEPARTMENT OF TRANSPORTATION
AND PURDUE UNIVERSITY

QUALITY ASSESSMENT OF GEOGRIDS USED FOR SUBGRADE TREATMENT

Min Sang Lee
Graduate Research Assistant
School of Civil Engineering
Purdue University

Yoon Seok Choi
Graduate Research Assistant
School of Civil Engineering
Purdue University

Monica Prezzi
Professor of Civil Engineering
School of Civil Engineering
Purdue University
Corresponding Author

SPR-3225
Report Number: FHWA/IN/JTRP-2012/27
DOI: 10.5703/1288284315034

RECOMMENDED CITATION

Lee, M. S., Y. S. Choi, and M. Prezzi *Quality Assessment of Geogrids Used for Subgrade Treatment*. Publication FHWA/IN/JTRP-2012/27. Joint Transportation Research Program, Indiana Department of Transportation and Purdue University, West Lafayette, Indiana, 2012. doi: 10.5703/1288284315034.

CORRESPONDING AUTHOR

Prof. Monica Prezzi
School of Civil Engineering
Purdue University
(765) 494-5034
mprezzi@purdue.edu

ACKNOWLEDGMENTS

This research was funded with the support provided by the Indiana Department of Transportation through the Joint Transportation Research Program at Purdue University. The authors would like to thank the agency for the support. The authors are also very grateful for the support received from the Project Administrator and the Study Advisory Committee, Yigong Ji, Tom Duncan, Tom Harris, Nayyar Zia, Enass Zayed, and Scott Trammell, throughout the duration of the project and for their valuable comments and suggestions. Thanks are due to Nayyar Zia and Athar Khan for their valuable comments during this work.

JOINT TRANSPORTATION RESEARCH PROGRAM

The Joint Transportation Research Program serves as a vehicle for INDOT collaboration with higher education institutions and industry in Indiana to facilitate innovation that results in continuous improvement in the planning, design, construction, operation, management and economic efficiency of the Indiana transportation infrastructure. https://engineering.purdue.edu/JTRP/index_html

Published reports of the Joint Transportation Research Program are available at: http://docs.lib.purdue.edu/jtrp/

NOTICE

TECHNICAL REPORT STANDARD TITLE PAGE

1. Report No.	2. Government Accession No.	3. Recipient's Catalog No.
FHWA/IN/JTRP-2012/27		

4. Title and Subtitle	5. Report Date
Quality Assessment of Geogrids Used for Subgrade Treatment	December 2012
	6. Performing Organization Code

7. Author(s)	8. Performing Organization Report No.
Min Sang Lee, Yoon Seok Choi, Monica Prezzi	FHWA/IN/JTRP-2012/27

9. Performing Organization Name and Address	10. Work Unit No.
Joint Transportation Research Program Purdue University 550 Stadium Mall Drive West Lafayette, IN 47907-2051	
	11. Contract or Grant No. SPR-3225

12. Sponsoring Agency Name and Address	13. Type of Report and Period Covered
Indiana Department of Transportation State Office Building 100 North Senate Avenue Indianapolis, IN 46204	Final Report
	14. Sponsoring Agency Code

15. Supplementary Notes

Prepared in cooperation with the Indiana Department of Transportation and Federal Highway Administration.

16. Abstract

Geogrid reinforcements have been used by the Indiana Department of Transportation (INDOT) to construct stable subgrade foundations and to provide a working platform for construction over weak and soft soils. Use of geogrid reinforcement in a pavement system ensures a long-lasting pavement structure by reducing excessive deformation and cracking. The main objectives of this research were to evaluate the mechanical interaction between a subgrade soil and an aggregate base layer with and without a geogrid in place at the interface. A series of large-scale direct shear tests were performed to investigate the effects of geogrid properties, such as geogrid aperture area, junction strength, and tensile strength, on the interface shear strength of soil-geogrid-aggregate systems. The test results showed that the aperture size and junction strength of the geogrids were relatively important factors affecting the overall interface shear strength the most. The average values for the peak interface shear strength coefficient for the three normal stresses (50 kPa, 100 kPa and 200 kPa) considered in this study ranged from 0.96 to 1.48. In addition, the test results showed that the average peak interface shear strength coefficient increases with increases in the junction strength of the geogrid. The optimum aperture area of the geogrid was found to be equal to 825 mm^2 (1.4 in^2) for the subgrade soil and aggregate considered in this study. There was no significant correlation between the geogrid tensile strength at 2% strain and the average peak interface shear strength coefficient. The effect of the moisture content of the subgrade soil on the peak interface shear strength coefficient was also investigated. The peak interface shear strength coefficient for the subgrade soil sample prepared at the optimum moisture content and compacted to relative compaction values of 94–96% (R_{soil} = 95–96% and $R_{aggregate}$ = 94–95%) and tested under a normal stress of 100 kPa was 20% less than that for the subgrade soil sample prepared at a moisture content 4% above the optimum moisture content. Based on the results of the tests performed in this study, an aperture area requirement of 825 mm^2 (1.4 in^2) and a junction strength requirement of 11.5 kN/m (788 lb/ft) were suggested as preliminary guidelines for subgrade reinforcement systems. These requirements are only limited to the use of Type IV geogrid (INDOT specification 207.04) for subgrade reinforcement with aggregate No. 53.

17. Key Words	18. Distribution Statement
geogrid, direct shear test, subgrade stabilization, soil, aggregate	No restrictions. This document is available to the public through the National Technical Information Service, Springfield, VA 22161.

19. Security Classif. (of this report)	20. Security Classif. (of this page)	21. No. of Pages	22. Price
Unclassified	Unclassified	33	

Form DOT F 1700.7 (8-69)

EXECUTIVE SUMMARY

QUALITY ASSESSMENT OF GEOGRIDS USED FOR SUBGRADE TREATMENT

Introduction

The Indiana Department of Transportation (INDOT) has been using geogrid reinforcement for improving weak subgrades because in many cases use of geogrids and replacement of a portion of the weak soil with aggregates is a faster and more effective solution than chemical treatment. Geogrids provide reinforcement by laterally restraining the subbase, thereby improving the bearing capacity of the pavement system and decreasing the shear stresses on the subgrade soil. However, INDOT engineers have reported that contractors tend to choose the cheapest geogrids available on the market, barely meeting the few requirements included in INDOT specifications.

In section 918 of the INDOT standard specifications (Soil Fabrics), the requirements specified for geogrid material properties are the minimum ultimate tensile strength, tensile modulus, and aperture size and open area of geogrids. The required tensile modulus and tensile strength of geogrids lie within very broad ranges. Unlike other DOTs (such as those in Kansas, Ohio, West Virginia, and Kentucky), INDOT does not specify minimum junction strength values for geogrids. Geogrid junction strength is an important factor that influences the long-term performance of pavement subjected to repeated traffic loads, and therefore minimum requirements for it should be included in specifications.

In this study, large-scale direct shear tests were performed to evaluate the efficiency of geogrid reinforcement placed between an aggregate layer (#53 aggregate; classified as poorly graded gravel) and a subgrade soil layer (glacial till; classified as clay loam). Based on the test results, correlations between a geogrid reinforcement efficiency parameter and properties of geogrids were investigated.

Findings

Large-scale direct shear tests were performed on soil-geogrid-aggregate samples. The aggregate and subgrade soil layers were compacted at their optimum moisture contents (OMC) to relative compaction values of 93–98%. (R_{soil} = 94–98% and $R_{aggregate}$ = 93–96%). Eight brands of biaxial geogrids were selected and tested in this study. Values of the average peak interface shear strength coefficient α_{peak} varied from 0.96 to 1.48, depending on the brand of geogrid tested.

Correlations between average α_{peak} and properties of the geogrids tested were explored. The optimum aperture area was found to be 825 mm^2 (1.28 in^2), while the optimum normalized aperture area, defined as the ratio of the square root of the geogrid aperture area to the D_{50} of the aggregate, was equal to 4.7. The average peak interface shear strength coefficient increased with increases in the junction strength of the geogrids. However, no significant correlation was found between the geogrid tensile strength at 2% strain and average α_{peak} values. Thus, based on the large-scale direct shear tests results, the geogrid aperture area and junction strength are the parameters that determine the efficiency of the soil-geogrid-aggregate system.

The relationship between the average peak interface shear strength coefficient and geogrid property requirements of the specifications of Indiana, West Virginia, and Kentucky DOTs were also compared. With respect to the aperture area, INDOT requires a much smaller aperture area than the other DOTs, with the requirements of the other DOTs being closer to the optimum aperture area determined in this study. The tensile strength values of the tested geogrids satisfy the requirements of all DOTs. The geogrid junction strength and the average peak interface shear strength coefficient show a strong correlation. However, currently, INDOT specifications do not have a requirement for geogrid junction strength.

Based on the correlation found in this study, an aperture area requirement of 825 mm^2 (1.28 in^2) and a junction strength requirement of 11.5 kN/m (788 lb/ft) were suggested as preliminary guidelines to be implemented by INDOT. The recommendation is restricted to the use of geogrid for subgrade reinforcement (Type IV of INDOT specifications 207.04) with No. 53 aggregate.

Large-scale direct shear tests were also performed at moisture contents 2% and 4% higher than the OMC on samples compacted to relative compaction values of 94–96% (R_{soil} = 95–96% and $R_{aggregate}$ = 94–95%). The peak interface shear strength coefficient for tests performed at a moisture content 2% above the OMC was 1.49, while for tests performed at a moisture content 4% above the OMC, α_{peak} was equal to 1.99.

Implementation

This research found that the aperture area and junction strength of geogrids influence the efficiency of subgrade reinforcement systems. Based on the results of large-scale direct shear tests performed in this study, we proposed an aperture area requirement of 825 mm^2 (1.28 in^2) and a junction strength requirement of 11.5 kN/m (788 lb/ft). The recommendation is restricted to the use of geogrid for subgrade reinforcement (Type IV of INDOT specification 207.04) with No. 53 aggregate. For the geogrids tested, no correlations were observed between the average peak interface shear strength coefficient and other geogrid properties, such as tensile strength at 2% strain, tensile modulus, and ultimate strength. The effects of the aggregate and geogrid type and density and moisture content of the subgrade soil were also investigated in this study. An implementation project would provide valuable insights on the pullout resistance of geogrids in the field.

CONTENTS

1. INTRODUCTION 1
1.1 Background 1
1.2 Research Objectives 2
1.3 Scope and Organization 2

2. GEOGRID REINFORCEMENT FOR SUBGRADE 2
2.1 Introduction 2
2.2 Use of Geogrids in Subgrade Stabilization 2
2.3 Pavement Reinforcement Mechanism 3
2.4 Evaluation of Geogrids for Stabilizing Weak Subgrades 3
2.5 Geogrids 4

3. LARGE-SCALE DIRECT SHEAR TESTS 7
3.1 Introduction 7
3.2 Test Equipment and Procedure 7
3.3 Test Materials 8
3.4 Interface Shear Strength Coefficient 10
3.5 Test Results 10
3.6 Comparison with Specifications 17

4. CONCLUSIONS 26
4.1 Summary 26
4.2 Conclusions 26

REFERENCES 27

LIST OF TABLES

Table	Page
Table 2.1 Geogrid reinforcement property requirements for base and subbase reinforcement of pavement systems	5
Table 2.2 Geogrid property requirements—Type I (biaxial geogrid)	5
Table 2.3 Geogrid property requirements—Type II (uniaxial geogrid)	6
Table 2.4 Minimum junction strength requirements	7
Table 3.1 Properties of the subgrade soil (glacial till)	9
Table 3.2 Properties of the No. 53 aggregate	10
Table 3.3 Index properties of Tensar BX geogrids	11
Table 3.4 Index properties of Huesker geogrids	12
Table 3.5 Index properties of Synteen geogrids	12
Table 3.6 Peak shear strength and c-ϕ shear strength fitting parameters for the soil-aggregate samples tested with and without geogrid	18
Table 3.7 End-of-test shear strength and c-ϕ shear strength fitting parameters for the soil-aggregate samples tested with and without geogrid	18
Table 3.8 Peak interface shear strength coefficient α_{peak} at three different normal stress values	18
Table 3.9 End-of-test interface shear strength coefficient $\alpha_{end\text{-}of\text{-}test}$ at three different normal stress values	19
Table 3.10 Peak shear stress and secant friction angle for different geogrid placement	22
Table 3.11 Peak shear stress and peak interface shear strength coefficient for subgrade soil tested at different moisture contents under a normal stress of 100 kPa	23
Table 3.12 Peak shear stress and peak interface shear strength coefficient for different test materials tested under a normal stress of 100 kPa	24
Table 3.13 Material properties of geogrids and geogrid property requirements of DOTs' specifications	25
Table 3.14 Preliminary guidelines for geogrid property requirements	26

LIST OF FIGURES

Figure | Page

Figure 2.1 Construction procedure for soil-geogrid-aggregate systems 2

Figure 2.2 Schematic diagram illustrating the geosynthetic reinforcement mechanism 3

Figure 2.3 Geogrid components 6

Figure 3.1 Soil placed in the lower shear box and compacted in three layers 7

Figure 3.2 Geogrid placed over soil and secured to the shear box 8

Figure 3.3 Aggregate placed in the upper shear box and compacted in three layers 8

Figure 3.4 Load cell and LVDT positioned properly after the top plate cap is placed over the aggregate layer 8

Figure 3.5 Particle-size distribution curve for subgrade soil 9

Figure 3.6 Results of standard Proctor compaction tests for the subgrade soil 9

Figure 3.7 Particle-size distribution curves for the No. 53 aggregate 10

Figure 3.8 Results of standard Proctor compaction tests for the No. 53 aggregate 11

Figure 3.9 Geogrid specimens (Tensar BX) 13

Figure 3.10 Geogrid specimens (Huesker FORNIT) 13

Figure 3.11 Geogrid specimens (Synteen SF) 13

Figure 3.12 Results of large-scale direct shear tests (without geogrid): (a) shear stress vs. displacement behavior for the interfaces under three different normal stresses, (b) peak shear stress vs. the corresponding normal stress and (c) end-of-test stress vs. the corresponding normal stress 14

Figure 3.13 Results of large-scale direct shear tests (Tensar BX1200 Geogrid): (a) shear stress vs. displacement behavior for the interfaces under three different normal stresses, (b) peak shear stress vs. the corresponding normal stress and (c) end-of-test shear stress vs. the corresponding normal stress 15

Figure 3.14 Results of large-scale direct shear tests (Huesker FORNIT30 Geogrid): (a) shear stress vs. displacement behavior for the interfaces under three different normal stresses, (b) peak shear stress vs. the corresponding normal stress and (c) end-of-test shear stress vs. the corresponding normal stress 16

Figure 3.15 Results of large-scale direct shear tests (Synteen SF12 Geogrid): (a) shear stress vs. displacement behavior for the interfaces under three different normal stresses, (b) peak shear stress vs. the corresponding normal stress and (c) end-of-test shear stress vs. the corresponding normal stress 17

Figure 3.16 Effect of the geogrid junction strength (in the machine direction) on the peak interface shear strength coefficient (direct shear tests performed with normal stresses equal to 50, 100 and 200 kPa) 19

Figure 3.17 Effect of the geogrid junction strength (in the machine direction) on the end-of-test interface shear strength coefficient (direct shear tests performed with normal stresses equal to 50, 100 and 200 kPa) 19

Figure 3.18 Effect of the geogrid aperture area on the average peak interface shear strength coefficient 20

Figure 3.19 Effect of the geogrid normalized aperture area on the average peak interface shear strength coefficient 20

Figure 3.20 Effect of the geogrid normalized aperture length in the direction of shearing on the average peak interface shear strength coefficient 21

Figure 3.21 Effect of the geogrid tensile strength at 2% strain on the average peak interface shear strength coefficient 21

Figure 3.22 Effect of the geogrid junction strength (in the machine direction) on the average peak interface shear strength coefficient 22

Figure 3.23 Comparison of the direct shear test results for different geogrid placement (tested with Tensar BX4100, soil compacted at OMC = 16.4% to R = 94–95% and aggregate compacted at OMC = 8.2% to R = 93–95%) 22

Figure 3.24 Effect of moisture content of the subgrade soil on the direct shear test results (tested with Tensar BX4100 at 100 kPa of normal stress and soil compacted to R = 95–96% and aggregate compacted at OMC = 8.2% to R = 94–95%) 23

Figure 3.25 Direct shear test results for different materials (tested with Tensar BX1200 with soil compacted at the OMC to relative compaction values of 93–96% (R_{soil} = 94–95% and $R_{aggregate}$ = 93–95%) and a normal stress of 100 kPa) 23

Figure 3.26 Relation between geogrid aperture area, average peak interface shear strength coefficient and property requirements of DOTs' specifications 24

Figure 3.27 Relation between geogrid tensile strength at 2%, average peak interface shear strength coefficient and property requirements of DOTs' specifications 24

Figure 3.28 Relation between geogrid junction strength (in the machine direction), average peak interface shear strength coefficient and property requirements of DOTs' specifications 25

1. INTRODUCTION

1.1 Background

A stable subgrade foundation is important to ensure a long-lasting pavement structure without excessive deformation. The lack of strength and stiffness of some foundation soils can present serious problems that can affect the long-term performance of pavements. Problematic soils, such as clay and silt in areas with high ground water table, can be removed and replaced by properly compacted sandy soils. Soil stabilization methods have also been used to overcome the problem of weak subgrade soils. Portland cement, fly ash and lime are often used to stabilize weak soils with high moisture contents. Appropriate control of the moisture content and density of the compacted soil or soil mixture are essential for proper subgrade performance. However, in urban areas, health concerns due to dust migration may prevent the use of such stabilization methods.

The Indiana Department of Transportation (INDOT) currently uses several methods to construct subgrade foundations, including compaction, chemical treatment or modification, and mechanical reinforcement using geosynthetics. Compaction is usually the least expensive option and is used often to improve subgrade soils. However, when clay and silt soils are encountered in areas with relatively high ground water table, the optimum moisture content (OMC) and, thus, the relative compaction requirements cannot be achieved by compaction methods. For these reasons, chemical treatment and geogrid reinforcement have been the methods preferred by INDOT in these cases. Geogrid provides reinforcement by laterally restraining the subbase and improving the bearing capacity of the system, thereby decreasing shear stresses on the subgrade soil. In addition, use of geogrids and replacement of a portion of the weak soils with aggregate is a faster and cleaner process than chemical treatment.

According to INDOT's standard specifications (section 207), INDOT allows seven types of subgrade treatments to be used with either chemical modification or geogrid reinforcement (*1*). These are:

1. **Type I:** 16 in. (400 mm) chemical soil modification, 12 in. (300 mm) of the subgrade excavated and replaced with coarse aggregate No. 53, or by 24 in. (600 mm) of soil compacted to density and moisture requirements.
2. **Type IA:** 16 in. (400 mm) chemical soil modification or 12 in. (300 mm) of the subgrade excavated and replaced with coarse aggregate No. 53.
3. **Type II:** 8 in. (200 mm) chemical soil modification, 6 in. (150 mm) of the subgrade excavated and replaced with coarse aggregate No. 53, or 12 in. (300 mm) of soil compacted to density and moisture requirements.
4. **Type IIA:** 8 in. (200 mm) chemical soil modification or 6 in. (150 mm) of the subgrade excavated and replaced with coarse aggregate No. 53.
5. **Type III:** 6 in. (150 mm) of soil compacted to the density and moisture requirements, or 6 in. (150 mm) of subgrade excavated and replaced with coarse aggregate No. 53.
6. **Type IIIA:** 6 in. (150 mm) of subgrade excavated and replaced with coarse aggregate No. 53.
7. **Type IV:** 9 in. (225 mm) of the subgrade excavated and replaced with coarse aggregate No. 53, with a geogrid placed between the subgrade soil and the aggregate layer.

In constructing a subgrade foundation with geogrids (Type IV), a 9-inch-thick aggregate layer (typically No. 53 aggregate) is recommended (this is based on empirical observations of performance) to be placed on a layer of geogrid that is placed on a wet, weak soil.

The requirements for geogrid materials are given in section 918 of INDOT's standard specifications (*1*), specifying the minimum ultimate tensile strength (machine direction, cross-machine direction), tensile modulus (machine direction, cross-machine direction), aperture size, and open area of geogrids Type I (Biaxial Geogrid) and Type II (Uniaxial Geogrid). Currently, sixteen different types of geogrids from several manufacturers have been approved by INDOT and are being used in subgrade construction. The required tensile modulus and tensile strength of each geogrid lie within very broad ranges. For instance, four different types of geogrids, from even the same manufacturer, are classified under the same category of Type I, according to INDOT specifications. The properties of geogrids (e.g., tensile strength and tensile modulus) and the price of geogrids vary considerably. In addition, unlike the Kentucky DOT, INDOT specifications do not require any evaluation on the junction strength of geogrids. This is an important factor that affects the long-term performance of the pavement under the application of repeated traffic loads.

For these reasons, INDOT engineers have reported that contractors tend to choose the cheapest geogrids available in the market, barely meeting INDOT specifications. With poor quality geogrids, a reinforced road is not expected to perform well in the long term. Use of poor quality geogrids may result in poor interlocking of the aggregates in the geogrid apertures, leading to excessive deformation of the subgrade and cracking of pavements, possibly also due to rupture of the geogrid at the junctions. Field experience of INDOT engineers with geogrids has led to the observation that there is considerable variation in the performance of different geogrids.

In summary, INDOT has been utilizing geogrids for building subgrade foundations over the past ten years. Geogrid reinforcements resist the applied loads by means of interaction between different materials: subgrade soils and aggregates (which ideally should be interlocked in the geogrid apertures). As a result of this reinforcement, the pavement system should not exhibit excessive deformation and cracking. In order to understand the long-term performance of soil-geogrid-aggregate systems, we investigate in this report the interaction between the different materials (geogrid, soil and aggregate) used by INDOT in weak subgrade construction. As mentioned earlier, currently INDOT does not have a systematic study that would help to identify what type of geogrid and surrounding materials

should be selected to build a suitable subgrade foundation. This is the motivation for the present study.

1.2 Research Objectives

The main goal of this research was to obtain experimental data that could be useful to INDOT to improve its specifications regarding geogrid reinforcement of weak subgrade soils. To achieve this goal, the interaction of several geogrids approved by INDOT with soil and aggregate was evaluated by performing large-scale direct shear tests. Fundamental geogrid properties that affect the performance of soil-geogrid-aggregate systems were evaluated as well.

The objectives of this study were the following:

1. To identify the properties of geogrids that INDOT needs to examine before;
2. To approve geogrid products for subgrade foundation;
3. To evaluate the mechanical interaction of the geogrids approved by INDOT with soil and aggregate;
4. To provide INDOT with guidelines for use of geogrids in subgrade construction.

1.3 Scope and Organization

Large-scale direct shear tests were performed with eight different types of geogrids, a typical clayey soil [glacial till; classified as CL according to the USCS and A-4 according to AASHTO] from Indiana, and No. 53 aggregate. The results of the experimental tests performed are presented and discussed in this report. The report is organized into four chapters, as described below:

- Chapter 1 provides a brief introduction.
- Chapter 2 reviews the literature, provides general information about the geogrid materials used in this study and discusses the reinforcement mechanism of geogrids.
- Chapter 3 presents the large-scale direct shear test results.
- Chapter 4 presents the conclusions of this study.

2. GEOGRID REINFORCEMENT FOR SUBGRADE

2.1 Introduction

A subgrade is typically reinforced by placing a geogrid at the subgrade/subbase or subgrade/base interface to improve the ability of the weak subgrade to withstand traffic loads without excessive deformation. Geogrids provide reinforcement by laterally restraining the base or subbase and improve the bearing capacity of the system, thus decreasing shear stresses on the weak subgrade. In addition, the confinement provided by geogrids improves the distribution of the vertical stress over the subgrade and decreases vertical subgrade deformation. The proper ratio of geogrid aperture size to aggregate grain size is an important factor affecting the performance of geogrid reinforcement systems (*2,3*).

Figure 2.1 shows schematically the typical construction procedure for geogrid reinforcement used in roadway applications by INDOT. The construction procedure for geogrid reinforcement is as follows:

1. Remove the weak surface soil (about 9 in.) using a bulldozer;
2. Place a layer of geogrid;
3. Place an aggregate layer (about 9 in.) in one lift;
4. Compact the aggregate layer.

2.2 Use of Geogrids in Subgrade Stabilization

The uses of geogrid in a pavement system are to (a) aid construction over soft subgrades, (b) improve or extend the pavement service life, and (c) reduce the structural cross section of the pavement for a given service life (*4,5*). The major functions of geosynthetics (geosynthetic is a general term used to describe several reinforcement products, including geogrids and geotextiles) are separation, reinforcement, filtration, and drainage (*6*). Two of the primary functions of geosynthetics are separation and reinforcement.

Geosynthetics perform a separation function by preventing contamination of the base coarse aggregate with fine soil particles of the soft subgrade [e.g., Lawson (*7*) indicated that contamination happens for soft subgrade soil with a California Bearing Ratio (CBR) $<3\%$]. Intermixing occurs by either the aggregate being forced into the subgrade by the action of the applied loads or by migration of the subgrade soil particles into the aggregate layer. Under the applied loads, such as those from vehicle wheels, the aggregate layer deforms. Milligan et al. (*8*) explained that when vertical loads are applied to a coarse-grained soil layer, high horizontal stresses develop within that layer. In the absence of a geotextile separator, outward shear stresses occur on the surface of the subgrade. The presence of the outward shear stress reduces the bearing

Figure 2.1 Construction procedure for soil-geogrid-aggregate systems.

capacity of the subgrade. Thus, fines are then able to migrate from the subgrade soil to the base course. Even though, the ability of a geogrid to separate two materials is less than that of a geotextile, geogrids can to some extent provide some measure of separation. However, the primary function of geogrids used in subgrade stabilization is reinforcement. The reinforcement mechanisms of geogrids are discussed next in section 2.3.

2.3 Pavement Reinforcement Mechanism

Reinforcements provide lateral restraint and improve the bearing capacity of reinforced systems (*9*). Carroll et al. (*10*) discussed the reinforcement mechanisms of geogrids used in paved roads. They found that geogrid reinforcement reduces permanent deformations in flexible pavement systems and allows up to a 50% reduction in the required thickness of a granular base based on equal load-deformation performance. Webster et al. (*11*) performed studies on geogrid reinforcement of flexible pavements for light aircraft. They indicated that geogrid reinforcement, which should be placed between the aggregate and subgrade layers for best performance, improves the performance of the pavement systems as a whole. Full-scale tests have verified that for California Bearing Ratio (CBR) strengths in the range of 1.5 to 5.0%, geogrid reinforced pavements can carry about 3.5 times more traffic load repetitions than non-reinforced pavements before a rut depth of 37 mm is reached (*11*).

2.3.1 Lateral Restraint

Horizontal reinforcements, such as geogrids, reduce the horizontal deformations of the base course and the subgrade soil at the interface (*12*). Improved lateral confinement results in an increase in the stiffness of the base course materials. The lateral restraint mechanism of a shear-resisting interface develops through shear interaction of the base course layer with the geogrid (geosynthetic) layer contained at the bottom of the base aggregate ((*9*); see Figure 2.2).

Traffic loads applied to the roadway surface create a lateral spreading motion of the base aggregate. Lateral tensile strains are created in the base just below the applied load as the material moves down and away from the load (*13*). Lateral movement of the base allows vertical strains to develop, leading to a permanent rut in the wheel path (*14*). Placement of a geogrid layer at the bottom of the base course allows shear interaction to develop between the aggregate and the geogrid as the base attempts to spread laterally. The mobilized shear load is transferred from the base aggregate to the geogrid. The relatively high stiffness of the geogrid helps delay the development of lateral tensile strains in the portion of the base adjacent to the geogrid. Lower lateral strains in the base produces less vertical deformation of the roadway surface.

The presence of a geogrid at the bottom of the base or subbase can also lead to a change in the state of stresses and strains in the subgrade. The geogrid layer increases the stiffness of the base or subbase. It distributes and decreases the vertical stresses on the subgrade beneath the base or subbase. As a result, geogrid reinforcement reduces shear strains in the subgrade.

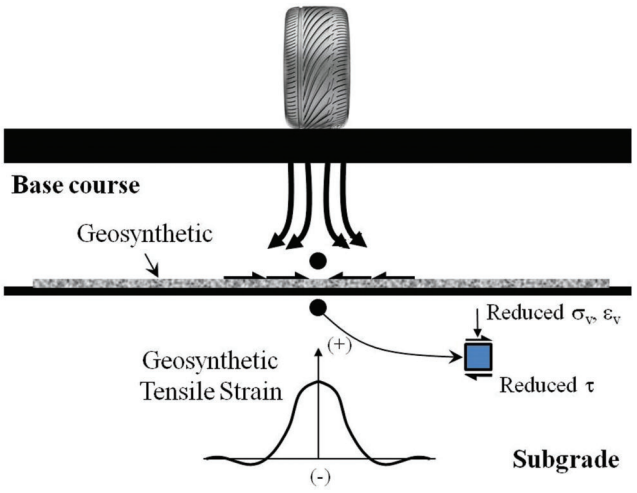

Figure 2.2 Schematic diagram illustrating the geosynthetic reinforcement mechanism (modified from (*9*)).

2.3.2 Improved Bearing Capacity

Use of geogrid over soft subgrade helps with the transfer of stresses from the relatively weak subgrade to the relatively strong base course material. The result is an improvement in the bearing capacity of the subgrade resulting from transfer of stresses at the geogrid-subgrade interface (*9*).

2.3.3 Tensioned Membrane Effect

The tensioned membrane effect is mobilized when the subgrade deforms. This type of reinforcing mechanism is especially important when laying a base course on soft subgrade with a limited load bearing capacity or when an unpaved road is subjected to repeated loading (*11*). As the subgrade deforms under loading, the geogrid stretches like a membrane. The loading is distributed over a wider area because of the vertical component of the tension, which develops in the geogrid. The membrane reinforcing mechanism allows for a reduction in the thickness of the base course required for initial construction. For this type of reinforcement mechanism to make a significant contribution, the subgrade CBR should be less than 3% (*15–17*). Many researchers indicated that geotextiles that possess a high modulus have greater load spreading ability for the same level of deformation (*17–20*).

2.4 Evaluation of Geogrids for Stabilizing Weak Subgrades

Based on both laboratory tests and full-scale field tests, many researchers have reported significant improvement

of the bearing capacity of pavements when geogrid reinforcement was used between the base course and the weak subgrade soil (*9,15,21*).

Barksdale et al. (*15*) assessed the performance of geogrids and geotextiles used in flexible pavements. Large-scale tests were performed in a test facility 4.9 × 2.4 m in plan using a 7 kN wheel loading moving at a speed of 4.8 km/h. Up to 70,000 repetitions of wheel loading were applied to the test sections. Pressure cells were installed in each of the test sections, and strain gages were used to measure strains in each layer of the flexible pavement sections and in the geogrids. These authors found that a minimum stiffness of 260 kN/m at 5% geogrid strain must be specified when geogrids are to be used as pavement reinforcement. Note that the stiffness of a geogrid at a specific geogrid strain is the secant modulus determined from a stress-strain (force per unit width vs. elongated strain) curve obtained from a tensile test (ASTM D6637 (*22*)). The results of Barksdale et al. (*15*) showed that when a geogrid was placed at the bottom of the base course there was a 52% reduction in permanent subgrade deformations. For weak subgrades (CBR $<$ 3%), total rutting in the base and subgrade could be reduced by 20 to 40% as a result of use of reinforcement. Some factors that could have influenced the results of their study are the magnitude and duration of the load applied.

Al-Qadi et al. (*21*) evaluated the performance of pavements with and without geotextile or geogrid reinforcement. Their tests were performed on eighteen pavement sections, including geotextile-stabilized and geogrid-reinforced sections. The pavement surface was dynamically loaded while displacements were recorded and monitored. The dynamic load, which was equal to approximately 550 kPa, was applied through a 300-mm-thick rigid plate at a frequency of 0.5 Hz. The loading simulated the dual load from an 80 kN axle with a tire pressure of 550 kPa. The experimental results showed that the geotextile-stabilized sections sustained 1.7 to over 3 times more the number of load repetitions than the control sections for 25 mm of permanent deformation. In the geogrid-reinforced sections, the granite aggregate material had penetrated into the silty sand subgrade material and the silty sand had migrated into the granite aggregate layer. The geotextile material was effective in preventing fines migration between the base course and subgrade layer.

Hass et al. (*2*) and Perkins et al. (*23*) showed that geogrid reinforcement increases the modulus of the base layer and improves the vertical stress distribution over the subgrade. Hufenus et al. (*24*) performed full-scale field tests on geogrid reinforced unpaved roads on soft subgrade. Hufenus et al. (*24*) also found that geogrid reinforcement increases the bearing capacity of the pavement and reduces rut formation.

Recently, Tang et al. (*3*) investigated the effects of geogrid properties on subgrade stabilization by performing large-scale direct shear tests, pullout tests and accelerated pavement tests (APT). Tang et al. (*3*) showed that the effectiveness of geogrid reinforcement is highly dependent on the physical and mechanical properties of the geogrids and on the properties of the interface between the geogrid and the surrounding materials.

Tang et al. (*25*) evaluated the interface efficiency of geogrid reinforcement by performing direct shear tests. Their results showed a good correlation between the tensile strength at 2% strain, junction strength and other parameters obtained from the large-scale direct shear tests. According to Tang et al. (*25*), relationships between the geogrid properties and the interface efficiency of the geogrid reinforcement are useful in the assessment of the quality of geogrids.

Koerner (*6*) proposed that an interface efficiency factor E_φ be calculated as the ratio of the tangent of the friction angles of the interface and soil according to:

$$E_\varphi = {}^{tan\delta}/_{tan\varphi} \tag{2.1}$$

where δ is the friction angle along the soil-geogrid interface, and ϕ is the friction angle of the soil. The interface efficiency factor for geotextiles varies from 0.6 to 1. However, the interface efficiency factor for geogrids can be greater than 1 (*26*). Based on the results of tests performed for four different types of geogrids interfacing with dense, crushed stone aggregate and silty sand, Tang et al. (*3*) found that the interface efficiency factor varies from 0.56 to 1.14.

The interface shear strength coefficient α is defined as the ratio of the shear strength of the subgrade soil system with the geogrid reinforcement to the shear strength of the subgrade soil system without the geogrid reinforcement, both measured under the same normal stress (*27–29*):

$$\alpha = {}^{\tau_{(\text{with geogrid})}}/_{\tau_{(\text{without geogrid})}} \tag{2.2}$$

where α = the interface shear strength coefficient; $\tau_{(\text{with geogrid})}$ = shear strength with the geogrid reinforcement; and $\tau_{(\text{without geogrid})}$ = shear strength without the geogrid reinforcement. The interface shear strength coefficient is also used to evaluate the efficiency of geogrid reinforcement. Liu et al. (*29*) performed large direct shear tests on samples of sand with and without reinforcement and reported interface shear strength coefficients varying from 0.92 to 1.01. Note that equations 2.1 and 2.2 are the same for frictional materials.

2.5 Geogrids

2.5.1 Geogrid Property Requirements

Table 2.1 provides the geogrid property requirements suggested in the GMA White Paper I (*30*), which defined geogrid types as Class 1 (base reinforcement) and Class 2 (subbase reinforcement). A Class 1 geogrid is placed directly beneath or within the aggregate base. A Class 2 geogrid is placed at the subgrade/subbase interface. The values for the geogrid property requirements in Table 2.1 represent default values that provide for sufficient geogrid reinforcement and survivability under

TABLE 2.1
Geogrid reinforcement property requirements for base and subbase reinforcement of pavement systems[1]

Property	Class 1 (base reinforcement)	Class 2 (subbase reinforcement) CBR ≥ 0.5
Ultimate Tensile Strength, UTS[2] (ASTM D4595 modified for geogrids)	12 (MD), 18 (XD) (kN/m)	12 (MD), 18 (XD) (kN/m)
Tensile Strength at Specified Strain[2] (ASTM D4595 modified for geogrids)	4 (MD), 6 (XD) at 2% strain (kN/m)	8 (MD), 13 (XD) at 2% strain (kN/m)
Geogrid Percent Open Area (COE CW-02215)	50 min. (%)	50 min. (%)
Junction Strength[3] (MD) (GRI GG2 modified to 10%/min.)	35 (N)	35 (N)
Ultraviolet Stability (Retained Strength[4]) (ASTM D4355)	50% (500 hrs)	50% (500 hrs)

SOURCE: (*30*).

NOTES:

[1]Values listed in Table 2.1 are the Minimum Average Roll Value (MARV), except for UV stability. (MARV=average value minus two standard deviations.)

[2]MD is the machine direction. XD is the cross-machine direction. MD is the direction in the plane of the fabric parallel to the direction of manufacture. In the field, the geogrid is placed such that the MD is parallel to the centerline of the roadway alignment.

[3]Junction strength is the strength required to maintain dimensional stability of the geogrid during deployment. It is not applicable to geogrid/geotextile composite products.

[4]Retained strength is the reduced tensile strength of geotextile after exposure to xenon arc radiation, moisture, and heat.

ASTM D4595, (*31*).

COECW-02215, (*32*).

ASTM D4355, (*33*).

most construction conditions. The design engineer may specify properties that are different from those listed in Table 2.1 based on engineering design and experience.

INDOT Standard Specifications (section 918.05) (*1*) specify the geogrid property requirements provided in Tables 2.2 and 2.3. The specifications include the geogrid aperture size, open area, tensile modulus and ultimate tensile strength of Type I (biaxial geogrid) and Type II (uniaxial geogrid) geogrids. INDOT has used fourteen approved Type I (biaxial) geogrids and two approved Type II (uniaxial) geogrids for geogrid reinforcement. However, the tensile modulus and tensile strength of each geogrid are in very broad ranges. In addition, there is considerable difference in the price of each geogrid, as well as in the geogrid properties, such as tensile strength and tensile modulus. For these reasons, INDOT engineers have reported that contractors tend to use the cheapest geogrids in the market that barely meet INDOT specifications. With poor quality geogrids, the reinforced subgrade and, hence, the pavement are expected to have poor long-term quality. Poor quality geogrids and poor interlocking between the aggregate and the geogrids will cause excessive deformation and cracking of the pavement in the long term.

2.5.2 Geogrid Survivability

Geogrids should meet the requirement of survivability. Survivability is defined as the resistance to mechanical damage during road construction and initial construction operations. The ability of a geosynthetic to survive installation and reasonable service loads must be assured. Table 2.1 shows recommended junction strength values for construction survivability based on tests performed to evaluate the junction strength of geogrids (Geosynthetics Research Institute (GRI) standard GG2 procedure (*35*)).

TABLE 2.2
Geogrid property requirements (INDOT Standard Specifications, section 918.05) —Type I (biaxial geogrid)

Property	Test method	Unit	Value, min.
Aperture	Calibrated	in (mm)	0.5 × 0.5 (13 × 13)
Open Area	COE CW-02215	%	>50.0, ≤80.0
Tensile Modulus, Machine Direction	ASTM D6637[1,2,3]	lb/ft (N/m)	10,000 (146,000)
Cross-Machine Direction		lb/ft (N/m)	10,000 (146,000)
Ultimate Strength, Machine direction	ASTM D6637[1,2,3]	lb/ft (N/m)	800 (11,670)
Cross-machine direction		lb/ft (N/m)	800 (11,670)

NOTES:

[1]Secant modulus at 5% elongation.

[2]Results for machine direction (MD) and cross-machine direction (XD) are required.

[3]Minimum average roll values shall be in accordance with ASTM D4759.

COECW-02215, (*32*).

ASTM D6637, (*22*).

TABLE 2.3
Geogrid property requirements (INDOT Standard Specifications, section 918.05)—Type II (uniaxial geogrid)

Property	Test method	Unit	Value, min.
Open Area	COE CW-02215	%	>50.0, ≤80.0
Tensile Modulus, Machine Direction	ASTM D6637[1,2]	lb/ft (N/m)	49,300 (720,000)
Creep Limited Strength, Machine Direction at 5% strain	ASTM D5362	lb/ft (N/m)	1090 (16,000)

NOTES:
[1]Secant modulus at 2% elongation.
[2]Minimum average roll values shall be in accordance with ASTM D 4759.
COECW-02215, (*32*).
ASTM D6637, (*22*).
ASTM D5362, (*34*).

Rainey and Barksdale (*36*) have indicated that installation damage to a geogrid is a function of the following:

- Geogrid thickness
- Compactive effort and lift thickness
- Type and weight of construction equipment used for fill spreading
- Grain size distribution of backfill
- Angularity of particles of backfill material
- Polymer used in the manufacture of geogrids
- Geogrid manufacturing process

2.5.3 Junction Strength of Geogrids

Geogrid ribs are classified as either longitudinal or transverse. Longitudinal ribs are parallel to the machine direction (roll direction), while the transverse ribs are perpendicular to the machine direction. The junctions in a geogrid are the points of intersection between longitudinal and transverse ribs. A section of a geogrid in plan view is shown in Figure 2.3.

Junction strength is usually defined in terms of the maximum single-junction strength (i.e., the force required to rip the junction apart) and obtained following the Geosynthetics Research Institute (GRI) standard GG2 procedure. It is calculated as:

$$J_{rib} = \sum_{i=1}^{n} J_i/n \tag{2.3}$$

where J_{rib} = average single-junction strength (in units of force); J_i = maximum single-junction strength of each junction (obtained experimentally); and n = total number of test specimens.

Alternatively, geogrid junction strength (Eq. (2.4)) is also reported in terms of force per unit width of the material, which is the force applied to the junction divided by the nominal aperture opening:

$$J_{grid} = (J_{rid})\left(n_{junctions\ per\ unit\ width}\right) \tag{2.4}$$

where J_{grid} = geogrid junction strength per unit width (force/unit width; meter or feet)); and $n_{junctions\ per\ width}$ = number of junctions per unit width.

Junction efficiency $E_{junction}$ is equal to the maximum single-junction strength divided by the maximum tensile strength of a single rib (average).

$$E_{junction} = \left(\frac{J_{rib}}{T_{rib}}\right) \times 100; \tag{2.5}$$

where T_{rib} = maximum tensile strength of a single rib (force/unit width).

Regardless of which definition is used, specifications of maximum junction strength are used for quality

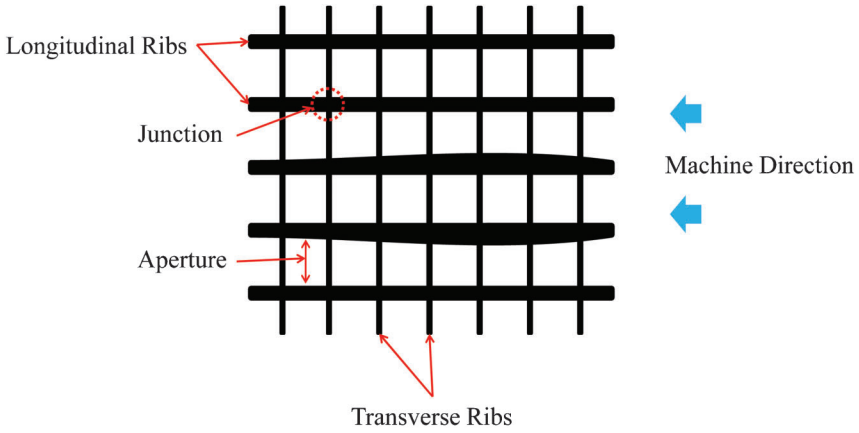

Figure 2.3 Geogrid components.

TABLE 2.4
Minimum junction strength requirements

DOT	Junction strength
Kansas DOT (Special Provision to the standard specification, section 1710)	25 lbs (111.2 N)
Ohio DOT (Supplemental Specification, section 861)	25 lbs (111.2 N)
West Virginia (Supplemental Specification, division 206)	765 lb/ft (11.16 kN/m) (Type 1) 1080 lb/ft (15.76 kN/m) (Type 2)
Kentucky DOT (Kentucky DOT memorandum, section 304)	765/1170 lb/ft (Type 1, MD/XD[1]) (11.16/17.07 kN/m) 1080/1780 lb/ft (Type 2, MD/XD[1]) (15.76/25.98 kN/m)

NOTES:
[1]Machine Direction (MD) × Cross-Machine Direction (XD). It is assumed that the MD is placed parallel to the centerline of the roadway alignment.
Kansas DOT, (*37*).
Ohio DOT, (*38*).
West Virginia, (*39*).
Kentucky DOT (*40*).

control and to ensure minimum constructability requirements. A minimum junction strength for roadway construction is required to maintain the integrity of the geogrid during shipment and placement. During roadway construction, the geogrid experiences high levels of localized stresses because aggregate material is placed, spread and compacted on top of the reinforcement. GMA White Report I (*30*) suggested a minimum junction strength value J_{rib} of 35 N (8 lbs), as shown in Table 2.1. However, Kansas and Ohio DOTs have increased this value to 110 N (25 lbs) based on their own experience with reinforced subgrade construction. West Virginia and Kentucky DOTs have minimum junction strength requirements in terms of geogrid junction strength per unit width. The minimum junction strength requirements specified by some DOTs are summarized in Table 2.4. The requirements for geogrid properties are only meant to provide guidelines regarding minimum requirements for the geogrid itself. Therefore, other subgrade design parameters (e.g., resilient modulus, CBR and shear strength) are needed for roadway design.

3. LARGE-SCALE DIRECT SHEAR TESTS

3.1 Introduction

Large-scale direct shear tests were performed in this study to evaluate the shear strength of the interface between subgrade soil and the aggregate base layer with and without geogrid reinforcement in place. Glacial till (CL) and No. 53 aggregate were used as subgrade and base material, respectively; these materials are most frequently used in weak subgrade reinforcement by INDOT. Eight types of geogrids from three different companies were selected for testing. Correlations between shear strength parameters and geogrids properties (tensile strength, junction strength and aperture size) were investigated. Based on the efficiency of the geogrids tested, the most relevant geogrid properties that affect the efficiency of the reinforced system were identified.

3.2 Test Equipment and Procedure

Large-scale direct shear tests were performed according to ASTM D5321 (*41*). The dimensions of the upper shear box are 300 mm × 300 mm, while those of the lower shear box are 300 mm × 450 mm. The size of the lower box is larger than that of the upper box to maintain a constant shearing area during the tests. Three different normal stresses (50 kPa, 100 kPa, and 200 kPa) were applied to the top of the samples. The rate of horizontal shear displacement was 1 mm/min. The large-scale direct shear test procedure was as follows:

1. The testing materials (subgrade soil and aggregate) were prepared at their optimum moisture contents.
2. The subgrade soil was compacted in the lower box in three layers (see Figure 3.1) to relative compaction values of 94–98%. Each layer was hammered a specified number of blows (280 blows for layer 1, 330 blows for layer 2, and 383 blows for layer 3). The number of blows was

Figure 3.1 Soil placed in the lower shear box and compacted in three layers.

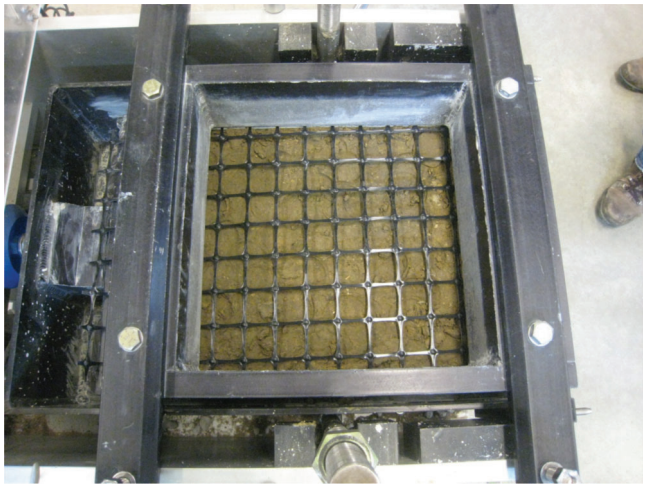

Figure 3.2 Geogrid placed over soil and secured to the shear box.

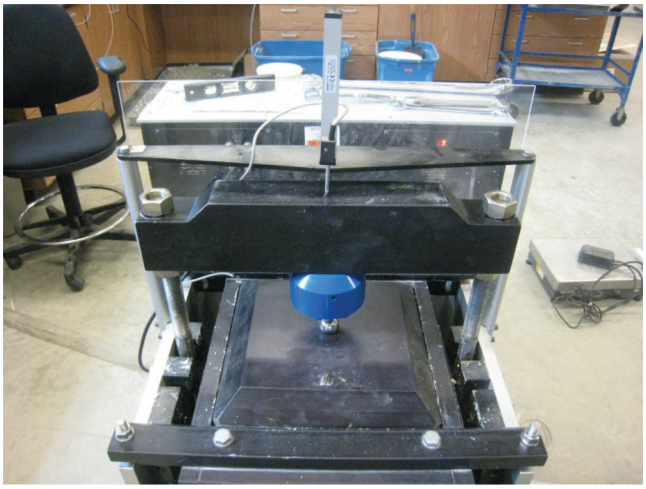

Figure 3.4 Load cell and LVDT positioned properly after the top plate cap is placed over the aggregate layer.

determined based on the Standard Proctor compaction effort.

3. The geogrid was installed on the compacted subgrade soil (Figure 3.2).
4. The upper box was placed and secured.
5. The base aggregate was compacted in the upper box. The aggregate was compacted in three layers (Figure 3.3) to relative compaction values of 93–96%. Each layer was hammered a specified number of blows (230 blows for layer 1, 250 blows for layer 2 and 370 blows for layer 3).
6. The top plate cap was placed over the aggregate, and the load cell and the LVDT were positioned (Figure 3.4).
7. The desired normal stress was applied on the sample. The normal stress was maintained until the vertical displacement was stabilized.
8. The lower box was then displaced at a constant rate of 1 mm/minute. The shear load, normal load, lateral and vertical displacement data were saved.
9. The test was terminated when the lateral displacement reached about 83 mm.

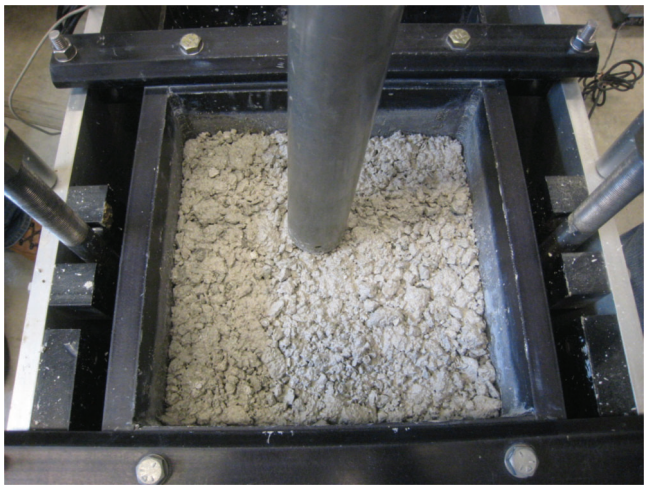

Figure 3.3 Aggregate placed in the upper shear box and compacted in three layers.

3.3 Test Materials

3.3.1 Subgrade Soil

The subgrade soil is a glacial till, which was classified as clay loam (CL) according to the Unified Soil Classification System (USCS, ASTM D2487 (*42*)) and as silty soil (A-4) according to the AASHTO soil classification (AASHTO M 145-91 (*43*)). The liquid limit, plastic limit and plasticity index of the subgrade soil were determined according to the Atterberg limits testing procedure (ASTM D4318-05 (*44*)). Figure 3.5 shows the particle-size distribution curve of the subgrade soil (ASTM D422-63 (*45*)). The subgrade soil properties are summarized in Table 3.1.

The optimum moisture content and maximum dry unit weight of the subgrade soil were obtained following the standard Proctor compaction test method (ASTM D698, Method A (*46*)). The subgrade soil optimum moisture content and maximum dry unit weight are 16.4% and 17.5 kN/m^3 (110.9 pcf), respectively, as shown in Figure 3.6.

3.3.2 Base Aggregate

The base material is No. 53 aggregate (crushed stone), which is the aggregate typically used in Indiana. The base aggregate (No. 53) is classified as poorly graded gravel (GP) according to the Unified Soil Classification System (USCS, ASTM D2487 (*42*)) and as stone fragments or gravel (A-1-a) according to the AASHTO soil classification (AASHTO M 145-91 (*43*)). The No. 53 aggregate properties and gradation are summarized in Table 3.2. INDOT standard specifications (section 904) specify the upper and lower limits for

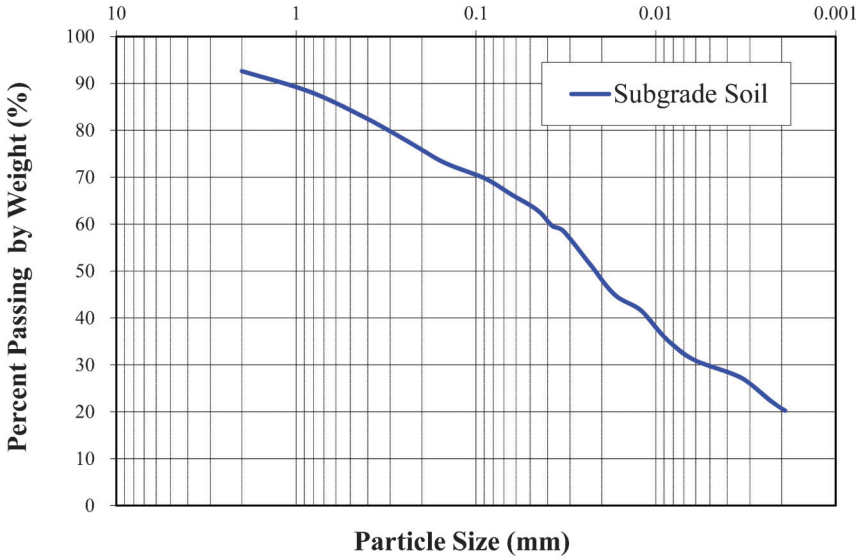

Figure 3.5 Particle-size distribution curve for subgrade soil.

TABLE 3.1
Properties of the subgrade soil (glacial till)

Sand (%)	Silt (%)	Clay (%)	LL (%)	PL (%)	PI (%)	Classification
32	48	20	30.5	21.3	9.2	CL (ASTM)/A-4 (AASHTO)

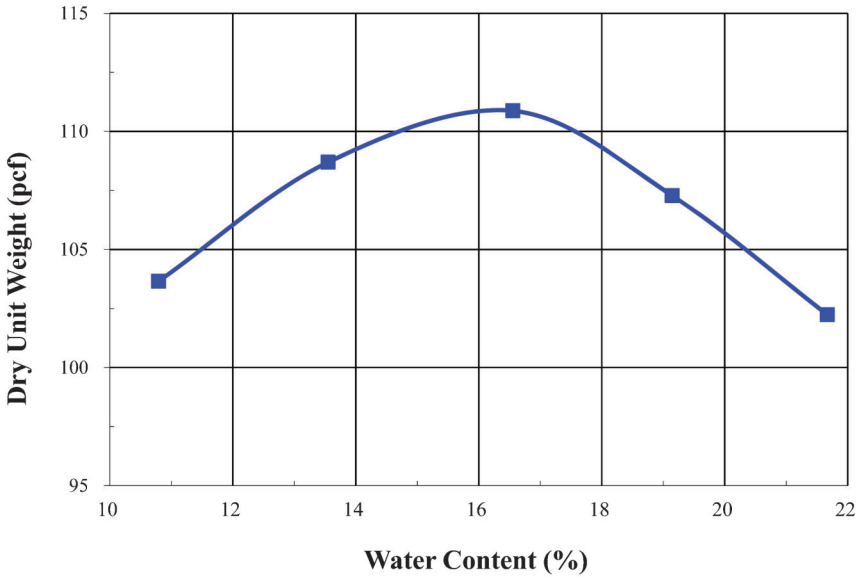

Figure 3.6 Results of standard Proctor compaction tests for the subgrade soil.

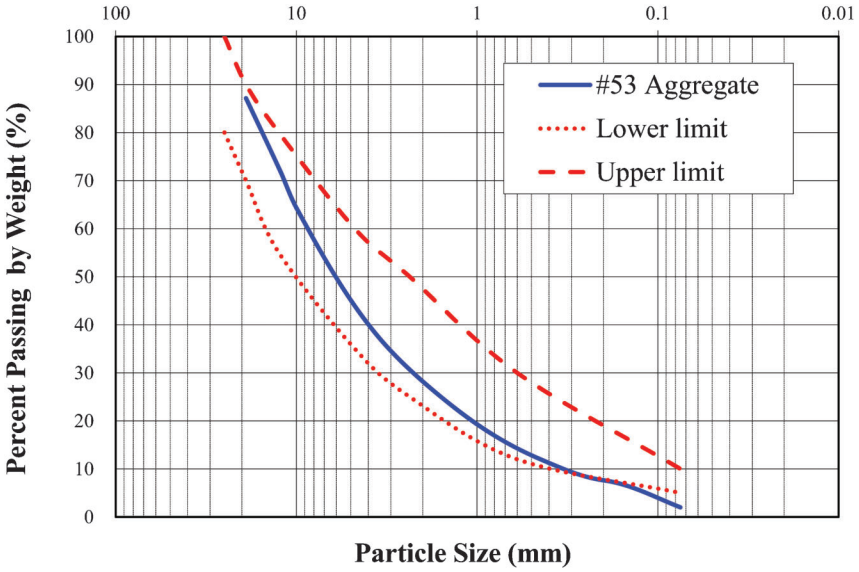

Figure 3.7 Particle-size distribution curves for the No. 53 aggregate.

the No. 53 aggregate particle-size distribution. These limits are shown in Figure 3.7. The particle-size distribution curve of the No. 53 aggregate used in this study lies between the upper and lower limits of the particle-size distribution specified by INDOT.

Standard compaction tests (ASTM D698, Method C (*46*)) were performed to obtain the optimum moisture content and maximum dry unit weight of the No. 53 aggregate. The No. 53 aggregate optimum moisture content and maximum dry unit weight are 8.2% and 21.6 kN/m^3 (139.6 pcf), respectively, as shown in Figure 3.8.

3.3.3 Geogrids

Eight brands of biaxial geogrids were selected for this study: Tensar BX1100, BX1200, and BX4100, FORNIT 20, 30, and 40/40, and Synteen SF11 and SF12. The index properties of the geogrids tested are provided in Tables 3.3, 3.4 and 3.5. Tensar BX geogrids (BX1100, BX1200, and BX4100) are produced using polypropylene or copolymers (see Figure 3.9). Huesker geogrids (FORNIT 20, 30, and 40/40) and Synteen geogrids (SF11 and SF12) are woven from polyester yarns and coated with PVC (see Figures 3.10 to 3.11). The aperture area and junction strength of the geogrid affect the frictional resistance at the interface since for efficient reinforcement performance, the aggregate particles need to get interlocked in the apertures of the geogrids. Tensar BX geogrids have relatively higher junction strength than the products supplied by the two other manufacturers (Huesker and Synteen). In addition, geogrids fabricated by the same manufacturer have different aperture sizes. Testing of geogrids with different properties allows one to compare and evaluate experimentally the performance of the different geogrid-reinforced systems.

TABLE 3.2
Properties of the No. 53 aggregate

Sieve size	Aggregates size (#53) (% passing)
3/4 in (19 mm)	87
1/2 in (12.5 mm)	73
3/8 in (9.5 mm)	63
No. 4 (4.75 mm)	44
No. 8 (2.36 mm)	30
No. 30 (600 μm)	9
No. 200 (75 μm)	2
PI	**NP**
Classification	GP (USCS) Stone fragments or gravel (AASHTO)

3.4 Interface Shear Strength Coefficient

The interaction of a geogrid with subgrade soil can be evaluated by comparing the shear strength at the interface measured in direct shear tests performed for various normal stresses with and without a geogrid in place. The interface shear strength coefficient α is often used to evaluate the effectiveness of geogrids used for subgrade reinforcement. The interface shear strength coefficient is defined as the ratio of the shear strength of the subgrade soil system with the geogrid reinforcement to the shear strength of the subgrade soil system without the geogrid reinforcement, both measured under the same normal stress (*27–29*).

3.5 Test Results

Figures 3.12 to 3.15 present the results of the large-scale direct shear tests performed in this study. In these

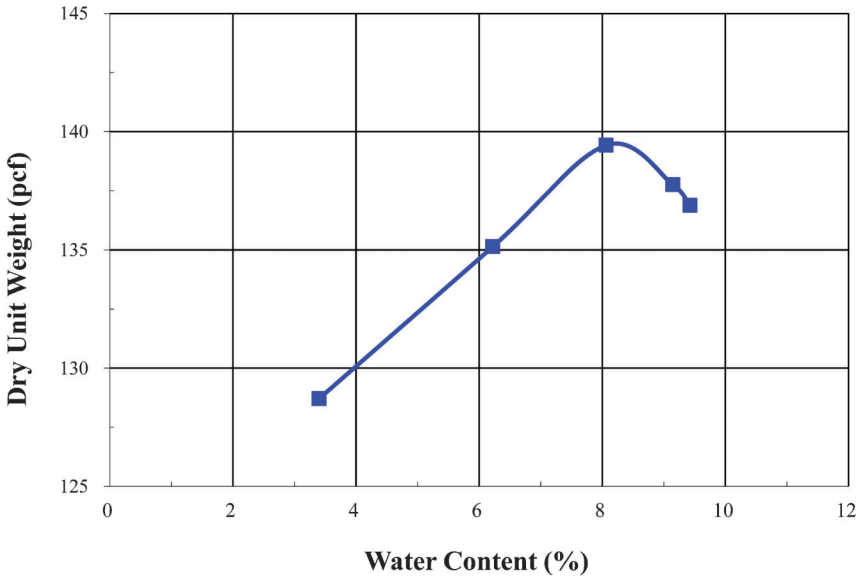

Figure 3.8 Results of standard Proctor compaction tests for the No. 53 aggregate.

TABLE 3.3
Index properties of Tensar BX geogrids[1]

Property	Geogrids		
	BX1100	**BX1200**	**BX4100**
Index Property	MD	MD	MD
Aperture size (mm)	25.0 (× 33.0)	25.0 (× 33.0)	33.0
Rib thickness (mm)	0.76	1.27	0.76
Tensile strength at 2% strain (kN/m)	4.1	6.0	4.0
Tensile strength at 5% strain (kN/m)	8.5	11.8	8.0
Ultimate tensile strength (kN/m)[2]	12.4	19.2	12.8
Junction strength (kN/m)[3]	11.53	17.86	11.90
Torsional stiffness (cm-kg/deg)[4]	3.2	6.5	2.8

NOTES:
[1]Available at http://www.tensarcorp.com/index.asp?id=70.
[2]Resistance to elongation is measured according to ASTM D6637. A geogrid specimen of is clamped and placed under a tensile force using a constant-rate of extension testing machine. The ultimate tensile strength is determined based on the tensile force required to rupture the specimen.
[3]Load transfer capability measured according to GRI-GG2-87.
[4]Resistance to in-plane rotational movement is measured by applying a 20 kg-cm moment to the central junction of a 9 in. × 9 in. specimen restrained at its perimeter (U.S. Army Corps of Engineers Methodology).

TABLE 3.4
Index properties of Huesker geogrids[1]

Property	Geogrids		
	FORNIT 20	**FORNIT 30**	**FORNIT 40**
Index property	MD	MD	MD
Aperture size (mm)	15.0	15.0	35.0
Rib thickness (mm)	—	—	—
Tensile strength at 2% strain (kN/m)	5.0	6.0	15.0
Tensile strength at 5% strain (kN/m)	9.0	12.0	32.0
Ultimate tensile strength (kN/m)[2]	13.0	25.0	40.0
Junction strength (kN/m)[3]	0.44	0.47	—
Torsional stiffness (cm-kg/deg)[4]	4.5	7.6	—

NOTES:
[1]Available at http://www.huesker.com/.
[2]Resistance to elongation is measured according to ASTM D6637.
[3]Load transfer capability measured according to GRI-GG2-87.
[4]Resistance to in-plane rotational movement (U.S. Army Corps of Engineers Methodology).

TABLE 3.5
Index properties of Synteen geogrids[1]

Property	Geogrids	
	SF11	**SF12**
Index property	MD	MD
Aperture size (mm)	25.0	25.0
Rib thickness (mm)	—	—
Tensile strength at 2% strain (kN/m)	7.7	7.7
Tensile strength at 5% strain (kN/m)	11.5	15.2
Ultimate tensile strength (kN/m)[1]	34.9	34.9
Junction strength (kN/m)[2]	0.87	0.87
Torsional stiffness (cm-kg/deg)[3]	—	—

NOTES:
[1]Available at http://www.synteen.com/products/base-reinforcement/.
[2]Resistance to elongation is measured according to ASTM D6637.
[3]Load transfer capability measured according to GRI-GG2-87.
[4]Resistance to in-plane rotational movement (U.S. Army Corps of Engineers Methodology).

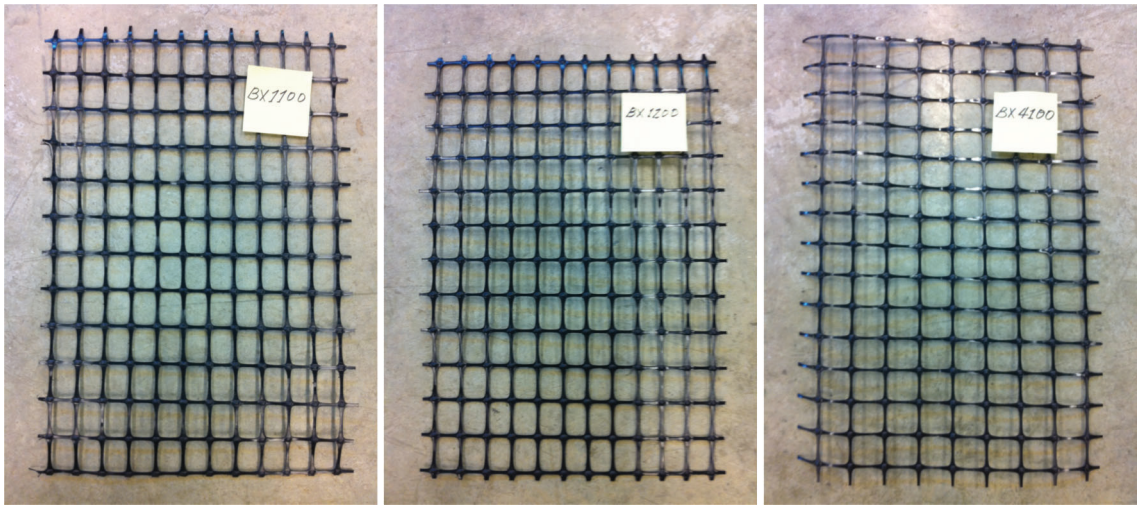

Figure 3.9 Geogrid specimens (Tensar BX).

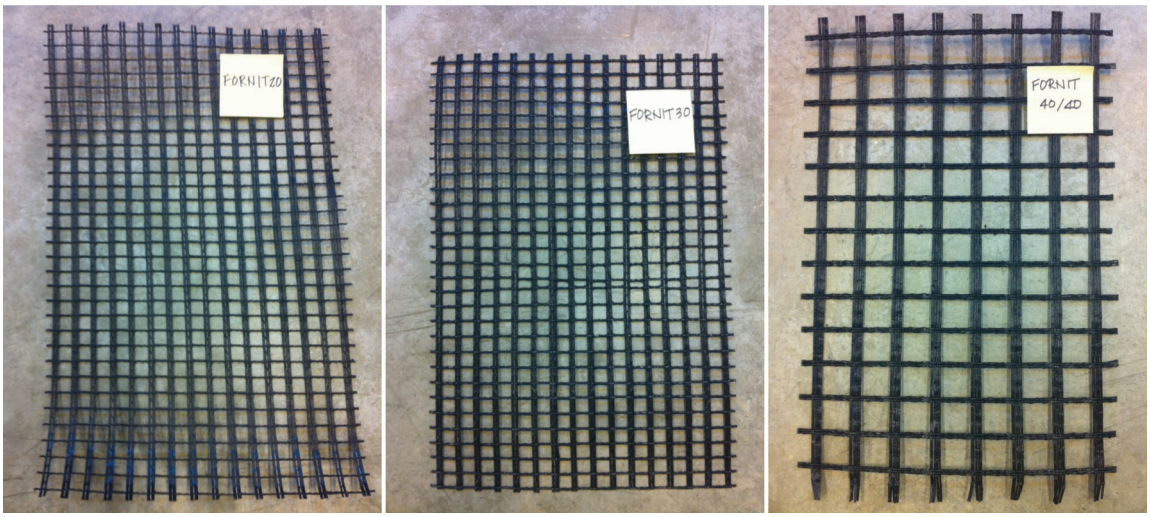

Figure 3.10 Geogrid specimens (Huesker FORNIT).

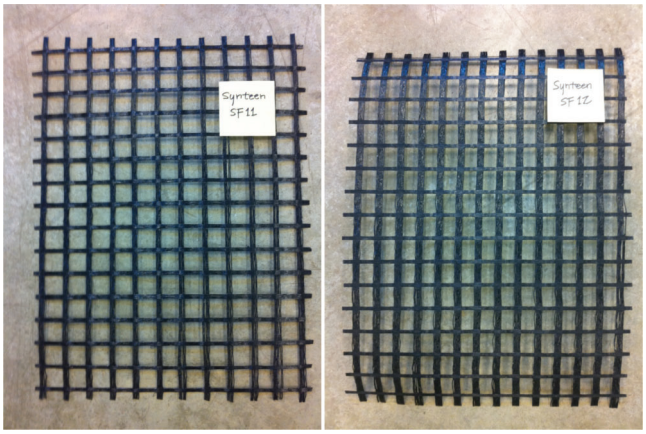

Figure 3.11 Geogrid specimens (Synteen SF).

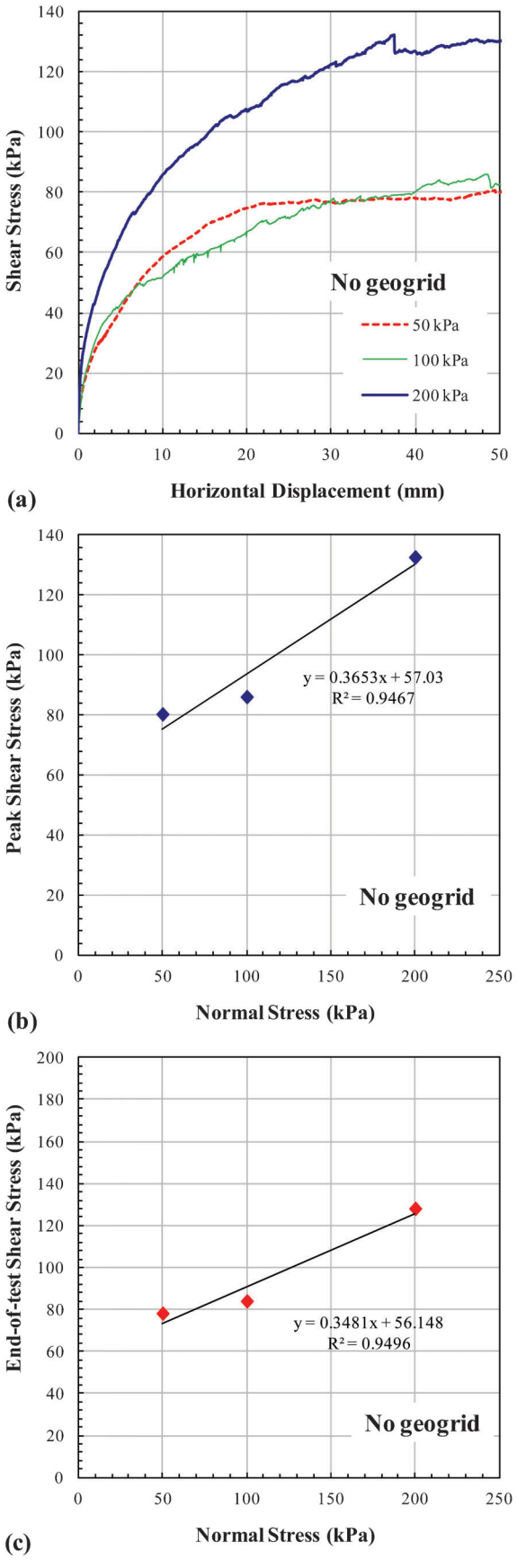

Figure 3.12 Results of large-scale direct shear tests (without geogrid): (a) shear stress vs. displacement behavior for the interfaces under three different normal stresses, (b) peak shear stress vs. the corresponding normal stress and (c) end-of-test stress vs. the corresponding normal stress.

figures, peak and end-of-test shear stresses are also plotted versus the corresponding normal stresses (50 kPa, 100 kPa and 200 kPa) to allow determination of the shear strength envelopes and the corresponding fitting parameters (cohesive intercept c and friction angle ϕ).

Figure 3.12 presents the variation of the shear stress developed along the horizontal shear plane during lateral displacement for the control interface of soil-aggregate without geogrid. Under a normal stress of 50 kPa, the peak shear strength in the shear stress-horizontal displacement curve is 80.3 kPa for the interface soil-aggregate without geogrid. For horizontal displacements greater than about 50 mm, the shear stresses developed along the horizontal shear plane reached a more or less steady value of 78.2 kPa at the end of the test.

From the plot of the peak shear strength versus the normal stress applied on the samples, fitting parameters (c = 57.0 kPa and friction angle = 20.1°) for the peak strength envelope were obtained for soil-aggregate samples without geogrid. Also, end-of-test fitting parameters for soil-aggregate samples without geogrid (c = 56.1 kPa and friction angle = 19.2°) were determined from the end-of-test shear strength envelope. Secant friction angles were also calculated from the peak and end-of-test shear strength envelopes (see Table 3.6 and Table 3.7). For a normal stress of 100 kPa, the peak and end-of-test secant friction angles for subgrade soil-aggregate without geogrid are equal to 40.7° and 40.0°, respectively.

Figures 3.13 to 3.15 show the variation of the shear stress with horizontal displacement and the peak and end-of-test shear strength envelopes for the geogrid (Tensar BX1200, Huesker FORNIT30, and Synteen SF12) reinforced soil-aggregate samples tested under three different normal stresses. Table 3.6 shows the c-ϕ shear strength fitting parameters corresponding to the peak shear strength envelopes for the soil-aggregate samples tested with and without geogrid. Table 3.7 provides the c-ϕ shear strength fitting parameters corresponding to the end-of-test shear strength envelopes for the soil-aggregate samples tested with and without geogrid.

The measured peak and end-of-test interface shear strength coefficients at three different normal stress values are summarized in Table 3.8 and 3.9. As can be seen in Table 3.8 and 3.9, the interface shear strength coefficient depends on the applied normal stress. At lower normal stresses, the materials are more dilative, while at higher normal stresses and larger strains, dilation is inhibited. Therefore, depending on the initial

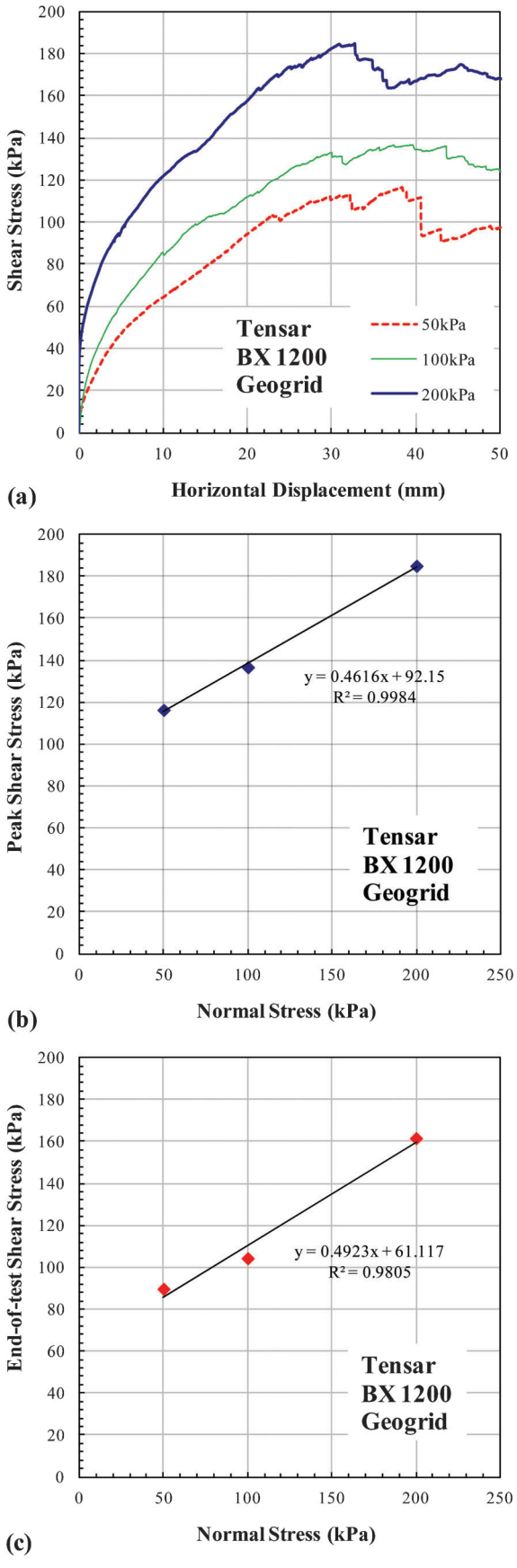

Figure 3.13 Results of large-scale direct shear tests (Tensar BX1200 Geogrid): (a) shear stress vs. displacement behavior for the interfaces under three different normal stresses, (b) peak shear stress vs. the corresponding normal stress and (c) end-of-test shear stress vs. the corresponding normal stress.

sample density and normal stress, the geogrid interaction mechanism is expected to be different. When dilation is suppressed, the effectiveness of the geogrid decreases since it depends on the degree of interlocking of the aggregate particles in the geogrid aperture. As the data in Table 3.9 shows, geogrids loose effectiveness at large strains. Figure 3.16 and Figure 3.17 show α_{peak} versus geogrid junction strength relationships for the various geogrids tested in this study. Overall, the variation in α_{peak} values is larger for the geogrids with lower junction strengths.

Figures 3.18 to 3.22 show the average peak interface shear strength coefficient versus the following properties of the eight geogrids tested: aperture size, junction strength (in the machine direction), and tensile strength. The Tensar BX1200 geogrid produced the greatest average peak interface shear strength. The aperture area and junction strength (in the machine direction) of the geogrid affected the overall average peak interface shear strength the most. Figure 3.18 indicates that the optimum aperture area of the geogrid is 825 mm^2 (1.28 in^2) for the subgrade soil and aggregate considered in this study. In addition, Figure 3.19 shows the average peak interface shear strength coefficient versus normalized aperture area, defined as the ratio of the square root of the geogrid aperture area to the D_{50} of the aggregate material. The optimum normalized aperture area is equal to 4.7. Figure 3.20 shows the average peak interface shear strength coefficient versus the aperture length of the geogrid in the direction of shearing normalized with respect to the D_{50} of the aggregate. The optimum normalized aperture length of the geogrid in the direction of shearing is equal to 5.4.

As shown in Figure 3.21, there is no direct correlation between the tensile strength at 2% strain and the average peak interface shear strength coefficient. Figure 3.22 shows that the average peak interface shear strength coefficient increases as the geogrid junction strength (in the machine direction) increases.

The shear stress and displacement response of a geogrid reinforced soil-aggregate system depends on various factors: the shear strength of soil or aggregate (related to intrinsic properties of the particles themselves, moisture content and density), the geogrid properties, and the test conditions. The effects of the moisture content of the subgrade soil, the placement of the geogrid on the direct shear box (attached either to the upper or lower box), the aggregate shear strength, and the soil shear strength on the shear stress vs. displacement response of the samples are discussed next.

There is no established procedure for the appropriate setup of a direct shear test device for testing of

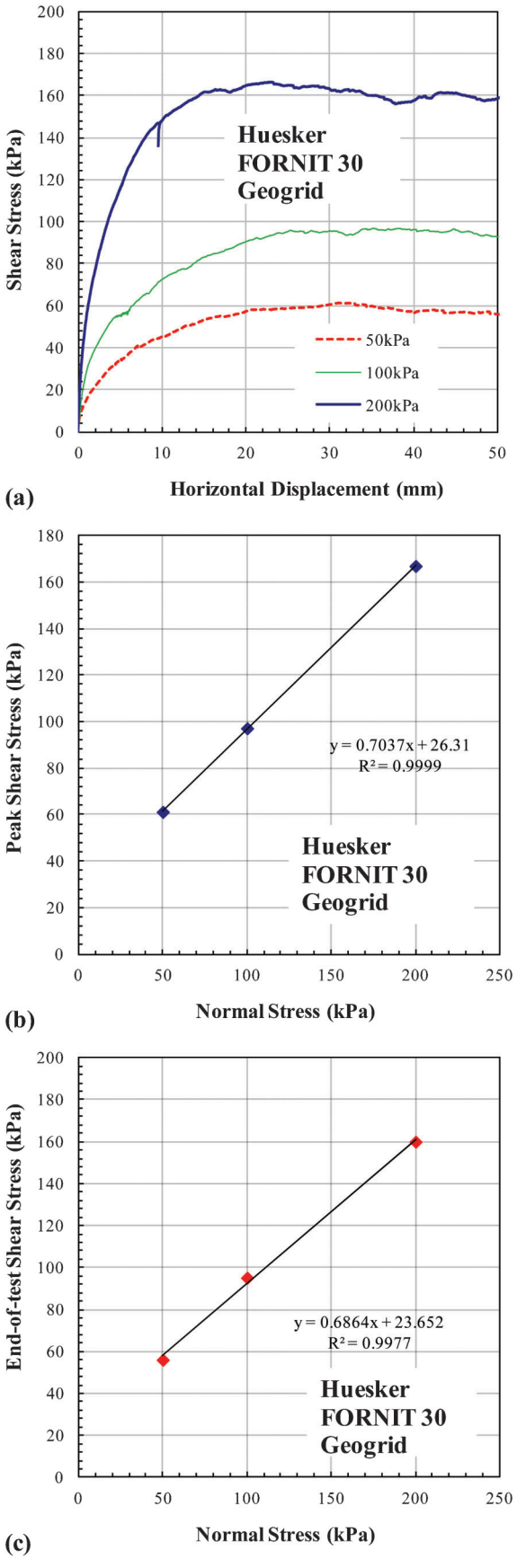

Figure 3.14 Results of large-scale direct shear tests (Huesker FORNIT30 Geogrid): (a) shear stress vs. displacement behavior for the interfaces under three different normal stresses, (b) peak shear stress vs. the corresponding normal stress and (c) end-of-test shear stress vs. the corresponding normal stress.

soil-geogrid interfaces. ASTM D5321 (standard for direct shear testing of soil-geosynthetic interfaces) (*40*) specifies only the minimum size of the shearing box. In this study, we also investigated the impact of the geogrid placement (either attached to the upper box or the lower box) on the measured interface shear strength. Glacial till (CL) and No. 53 aggregate were used in these tests as well. The soil and aggregate were compacted at their optimum moisture contents (OMC_{soil} = 16.4%; $OMC_{aggregate}$ = 8.2%) to relative compaction values of 93–95% (R_{soil} = 94–95%; $R_{aggregate}$ = 93–95%). Figure 3.23 shows a comparison of the direct shear test results for these two test conditions. For the same normal stress, relatively smaller shear strength was measured when the geogrid (Tensar BX4100) was attached to the upper shear box. Table 3.10 provides values for the peak shear stress and secant friction angle for tests performed with different geogrid placement in the box and a normal stress of 100 kPa. For a normal stress of 100 kPa, the peak shear strength values in the shear stress-horizontal displacement curves were 114.3 kPa for the test in which the geogrid was attached to the lower box and 104.6 kPa for the test in which the geogrid was attached to the upper box.

Figure 3.24 shows the results of the direct shear tests performed to assess the effect of the moisture content of the subgrade soil on the peak shear strength of the samples tested with and without geogrids in place. The subgrade soil samples were prepared at a moisture content of 2% and 4% wet of the standard Proctor optimum moisture content and compacted to relative compaction values of 94–96% (R_{soil} = 95–96%; $R_{aggregate}$ = 94–95%). For the same moisture content of the subgrade soil, the peak shear strength was larger for the samples prepared with a geogrid between the subgrade soil and the aggregate. This behavior was observed for all the samples prepared with the different moisture contents considered in this study. In addition, for both conditions (with and without geogrids), the peak shear strength at the interface decreases as the moisture content of the subgrade soil samples increases. Under an applied normal stress of 100 kPa, the interface peak shear strength coefficient (α_{peak} = 1.59) obtained from the tests performed at the optimum moisture content is 20% less than that (α_{peak} = 1.99) obtained for the samples tested at a moisture content 4% higher than the optimum moisture content (see Table 3.11).

Figure 3.25 shows a comparison of the peak shear strength at the interface for different materials tested at the OMC (OMC_{soil} = 16.4%; $OMC_{aggregate}$ = 8.2%) compacted to relative compaction values of 93–95%

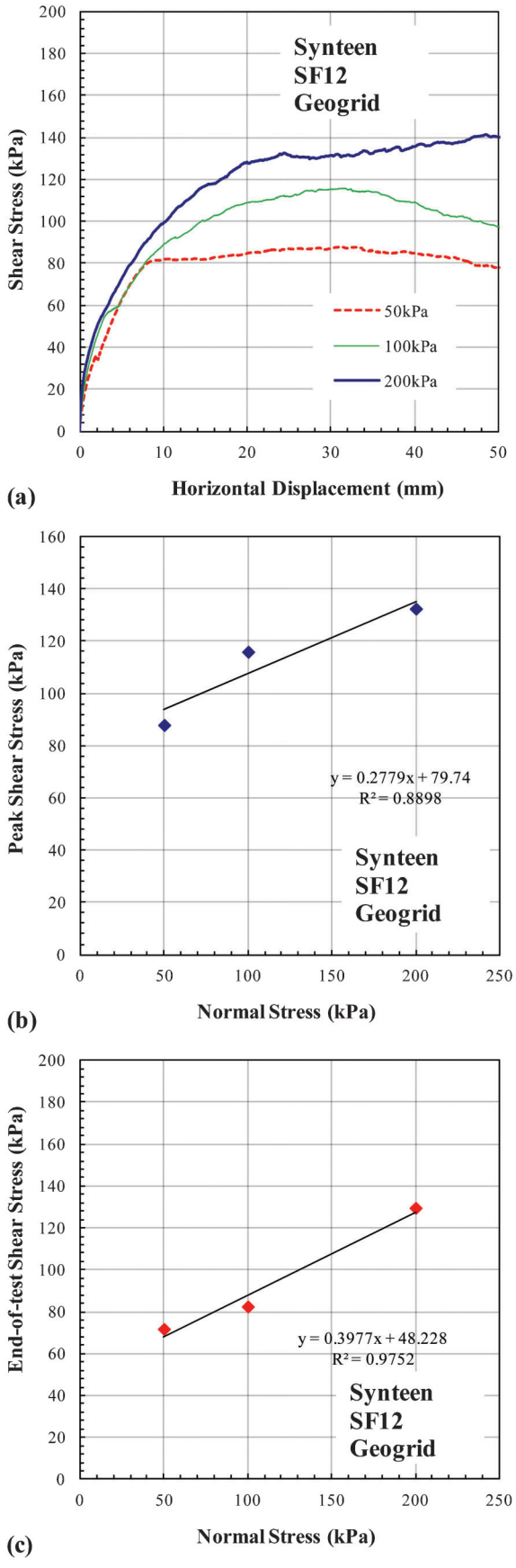

Figure 3.15 Results of large-scale direct shear tests (Synteen SF12 Geogrid): (a) shear stress vs. displacement behavior for the interfaces under three different normal stresses, (b) peak shear stress vs. the corresponding normal stress and (c) end-of-test shear stress vs. the corresponding normal stress.

(R_{soil} = 94–95%; $R_{aggregate}$ = 93–95%) with and without Tensar BX1200 geogrid in place for a normal stress of 100 kPa. The test conditions included only aggregate (both upper and lower shear box were filled with aggregate), only subgrade soil, and soil-aggregate. The results show that the shear strength at the interface for only aggregate is higher than that for only subgrade soil, both cases with Tensar BX1200 geogrid in place. However, the peak interface shear strength coefficient for the sample with only aggregate and geogrid is less than one (the value of α_{peak} is equal to 0.68). This means that placement of a geogrid between two layers of aggregate is detrimental to the interface shear strength. The test results show that use of Tensar BX1200 geogrid improves the shear strength at the interface when it is placed either between two layers of soil or between a layer of soil and a layer of aggregate. Values of the peak interface shear strength coefficient were found to be equal to 2.02 and 1.59 for the subgrade soil and the aggregate-soil samples, respectively, as shown in Table 3.12.

3.6 Comparison with Specifications

The results of the large-scale direct shear tests performed in this study show that the efficiency of geogrid reinforcement systems is related to the aperture area and the junction strength of the geogrids. In this section, we discuss requirements of geogrid properties in Indiana, West Virginia, and Kentucky DOTs' specifications so that reasonable property requirements can be proposed for INDOT specifications.

The relationships between the average peak interface shear strength coefficient and geogrid property requirements (aperture area, tensile strength at 2% strain, ultimate tensile strength, and junction strength in the machine direction) of Indiana, West Virginia, and Kentucky DOTs' specifications are shown in Figure 3.26 to Figure 3.28. Table 3.13 summarizes the properties of geogrids used in this study and the geogrid property requirements in the DOTs' specifications. The peak interface shear strength coefficients provided in Figure 3.26 to Figure 3.28 and Table 3.13 are the average values of the peak interface shear strength coefficients obtained for the three normal stresses (50 kPa, 100 kPa and 200 kPa) considered in this study.

With respect to the aperture area, INDOT requires a much smaller aperture area than the other DOTs' (Figure 3.26). The other DOTs' requirements are closer to the optimum aperture area (825 mm^2 = 1.28 in^2)

TABLE 3.6
Peak shear strength and c-ϕ shear strength fitting parameters for the soil-aggregate samples tested with and without geogrid

	Peak shear stress, τ [kPa]			Fitting parameters		Secant friction angle σ_n = 100 kPa
Geogrid	**σ_n = 50 kPa**	**σ_n = 100 kPa**	**σ_n = 200 kPa**	**ϕ**	**c**	**ϕ_{secant}**
No Geogrid	80.3	86.1	132.6	20.1	57.0	40.7
FORNIT 20	70.2	94.8	119.9	17.7	57.6	43.5
FORNIT 30	61.2	97.1	166.9	35.1	26.3	44.2
FORNIT 40/40	84.4	114.7	143.8	23.2	53.4	48.9
BX1100	117.9	129.5	142.0	8.8	111.6	52.3
BX1200	116.3	136.7	185.0	24.7	92.2	53.8
BX4100	113.6	114.3	151.6	15.1	95.0	48.8
SF11	101.1	104.6	127.8	10.5	89.5	46.3
SF12	88.0	116.0	132.5	15.5	79.7	49.2

NOTE: Glacial till (CL) soil compacted at OMC = 16.4% to R = 94–98% and No. 53 aggregate (GP) compacted at OMC = 8.2% to R = 93–96%.

TABLE 3.7
End-of-test shear strength and c-ϕ shear strength fitting parameters for the soil-aggregate samples tested with and without geogrid

	End-of-test shear stress, τ [kPa]			Fitting parameters		Secant friction angle σ_n = 100 kPa
Geogrid	**σ_n = 50 kPa**	**σ_n = 100 kPa**	**σ_n = 200 kPa**	**ϕ**	**c**	**ϕ_{secant}**
No geogrid	78.2	84.0	128.1	19.2	56.1	40.0
FORNIT 20	62.8	88.7	120.9	20.7	46.7	41.6
FORNIT 30	56.1	95.2	160.0	34.5	23.7	43.6
FORNIT 40/40	77.9	111.6	141.5	22.1	63.0	48.1
BX1100	85.1	99.5	112.7	10.0	78.5	44.9
BX1200	89.7	104.3	161.6	26.2	61.1	46.2
BX4100	84.8	103.5	129.0	16.1	72.0	46.0
SF11	89.4	92.6	124.8	14.0	73.3	42.8
SF12	71.8	82.5	129.6	21.7	48.2	39.5

NOTE: Glacial till (CL) soil compacted at OMC = 16.4% to R = 94–98% and No. 53 aggregate (GP) compacted at OMC = 8.2% to R = 93–96%.

TABLE 3.8
Peak interface shear strength coefficient α_{peak} at three different normal stress values

	Peak interface shear strength coefficient α_{peak}			
Geogrid	**σ_n = 50 kPa**	**σ_n = 100 kPa**	**σ_n = 200 kPa**	**Average α_{peak}**
FORNIT 20	0.87	1.10	0.90	0.96
FORNIT 30	0.76	1.13	1.26	1.05
FORNIT 40/40	1.05	1.33	1.08	1.16
BX1100	1.47	1.50	1.07	1.35
BX1200	1.45	1.59	1.40	1.48
BX4100	1.41	1.33	1.14	1.30
SF11	1.26	1.22	0.96	1.15
SF12	1.10	1.35	1.00	1.15

NOTE: Glacial till (CL) soil compacted at OMC = 16.4% to R = 94–98% and No. 53 aggregate (GP) compacted at OMC = 8.2% to R = 93–96%.

TABLE 3.9
End-of-test interface shear strength coefficient $\alpha_{end\text{-}of\text{-}test}$ at three different normal stress values

Geogrid	End-of-test interface shear strength coefficient $\alpha_{end\text{-}of\text{-}test}$			Average $\alpha_{end\text{-}of\text{-}test}$
	σ_n = 50 kPa	σ_n = 100 kPa	σ_n = 200 kPa	
FORNIT 20	0.80	1.06	0.93	0.93
FORNIT 30	0.70	1.13	1.25	1.03
FORNIT 40/40	0.97	1.33	1.10	1.13
BX1100	1.06	1.18	0.88	1.04
BX1200	1.12	1.24	1.26	1.21
BX4100	1.06	1.23	1.01	1.10
SF11	1.11	1.10	0.97	1.06
SF12	0.89	0.98	1.01	0.96

NOTE: Glacial till (CL) soil compacted at OMC = 16.4% to R = 94–98% and No. 53 aggregate (GP) compacted at OMC = 8.2% to R = 93–96%.

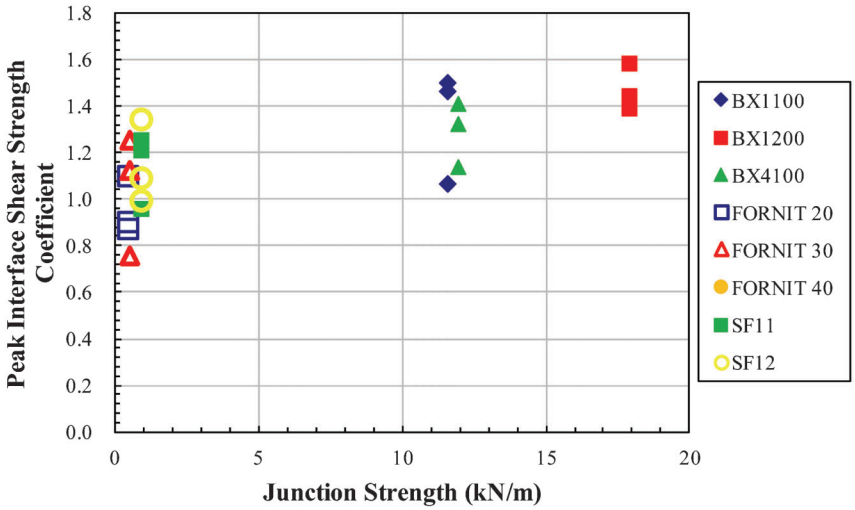

Figure 3.16 Effect of the geogrid junction strength (in the machine direction) on the peak interface shear strength coefficient (direct shear tests performed with normal stresses equal to 50, 100 and 200 kPa).

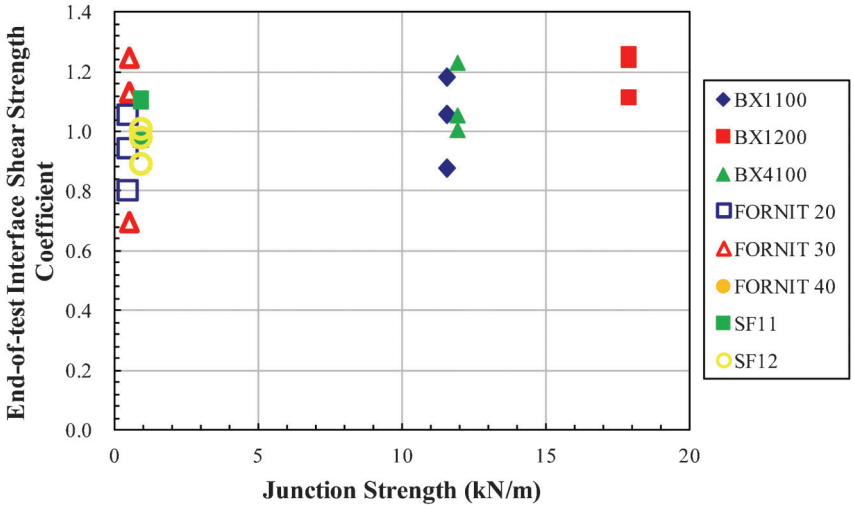

Figure 3.17 Effect of the geogrid junction strength (in the machine direction) on the end-of-test interface shear strength coefficient (direct shear tests performed with normal stresses equal to 50, 100 and 200 kPa).

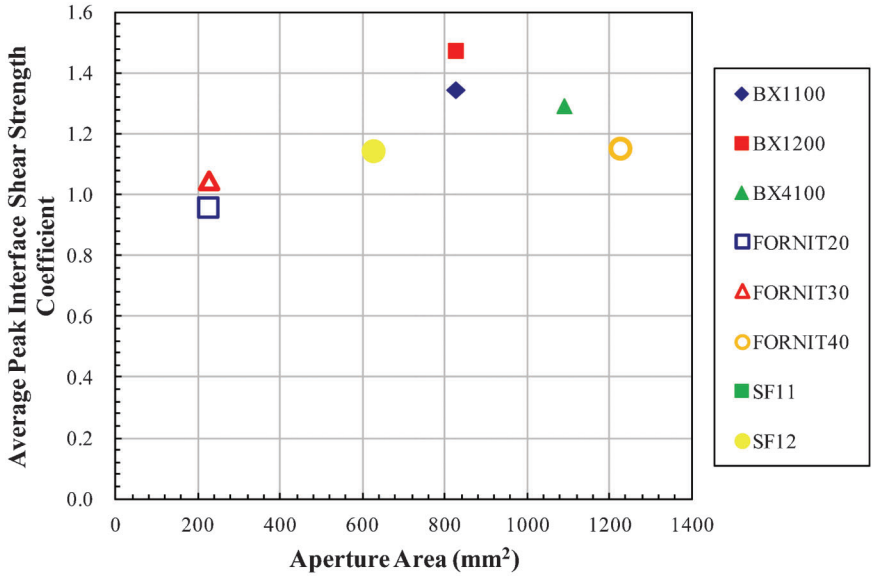

Figure 3.18 Effect of the geogrid aperture area on the average peak interface shear strength coefficient.

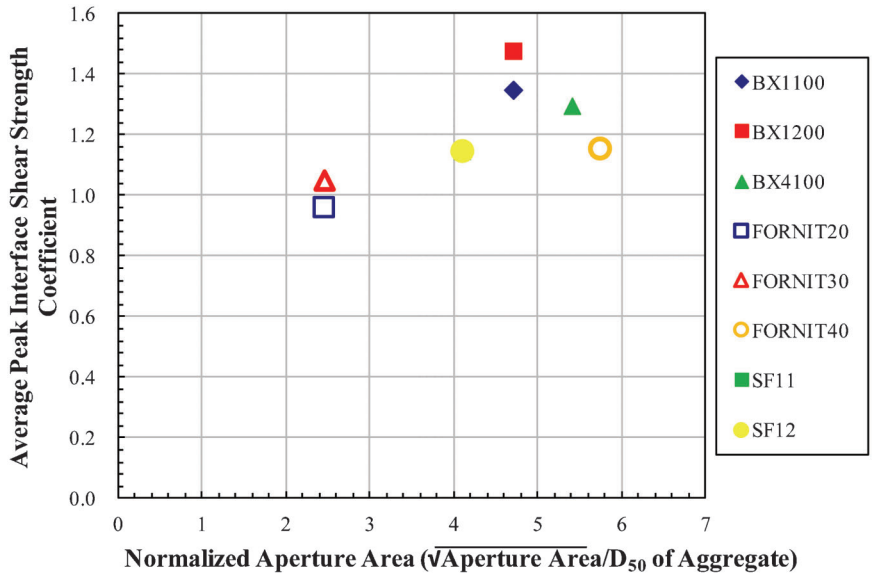

Figure 3.19 Effect of the geogrid normalized aperture area on the average peak interface shear strength coefficient.

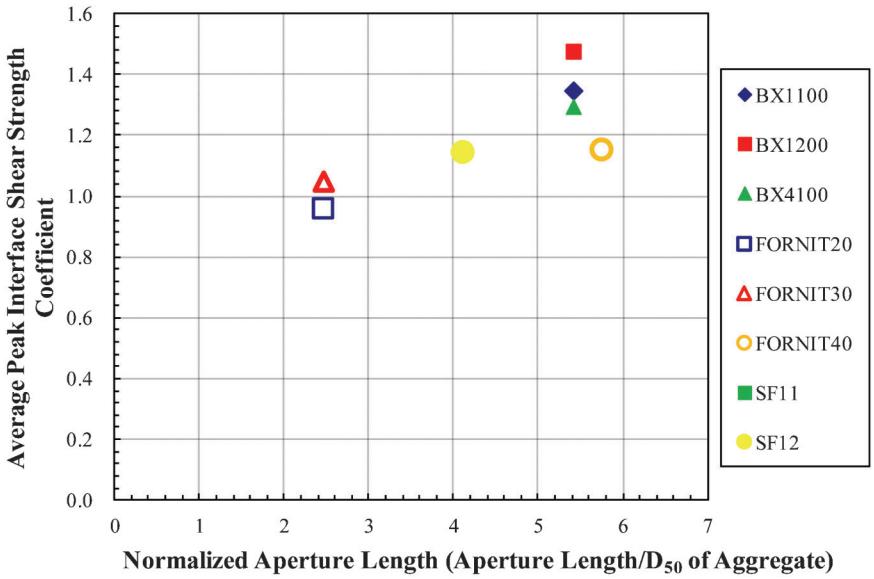

Figure 3.20 Effect of the geogrid normalized aperture length in the direction of shearing on the average peak interface shear strength coefficient.

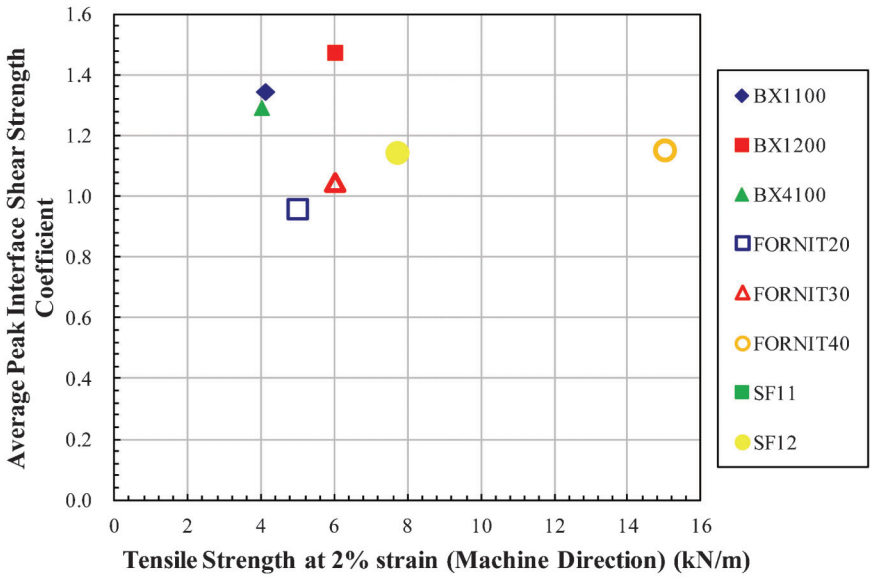

Figure 3.21 Effect of the geogrid tensile strength at 2% strain on the average peak interface shear strength coefficient.

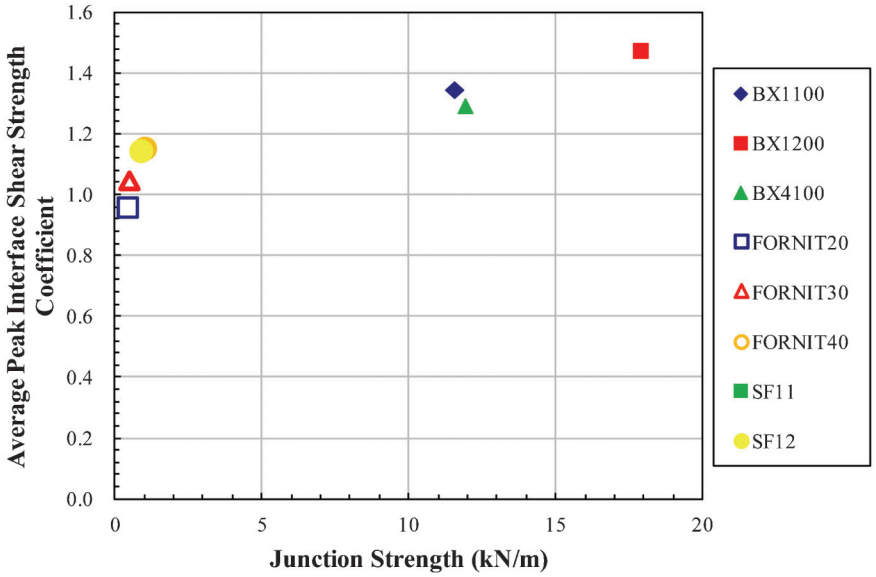

Figure 3.22 Effect of the geogrid junction strength (in the machine direction) on the average peak interface shear strength coefficient.

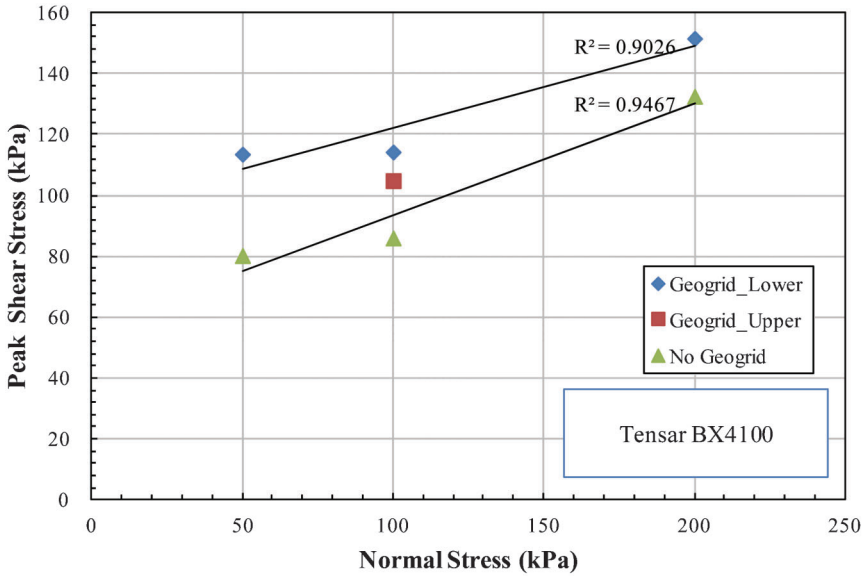

Figure 3.23 Comparison of the direct shear test results for different geogrid placement (tested with Tensar BX4100, soil compacted at OMC = 16.4% to R = 94–95% and aggregate compacted at OMC = 8.2% to R = 93–95%).

TABLE 3.10
Peak shear stress and secant friction angle for different geogrid placement

Geogrid placement	Peak shear stress τ [kPa] σ_n = 100 kPa	Secant friction angle ϕ_{secant} σ_n = 100 kPa
Without geogrid	86.1	40.7
Tensar BX4100 (geogrid attached to the lower box)	114.3	48.8
Tensar BX4100 (geogrid attached to the upper box)	104.6	46.3

NOTE: Glacial till (CL) soil compacted at OMC = 16.4% to R = 94–95% and No. 53 aggregate (GP) compacted at OMC = 8.2% to R = 93–95%.

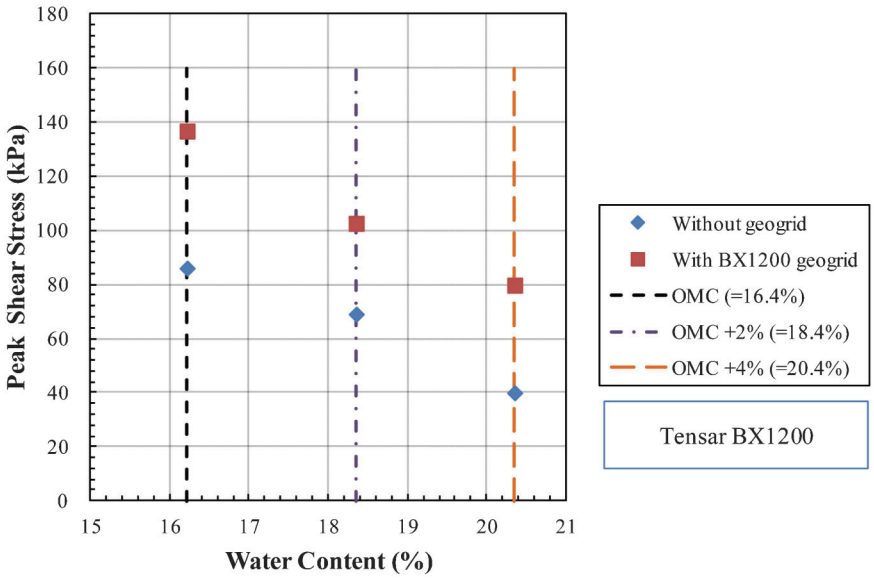

Figure 3.24 Effect of moisture content of the subgrade soil on the direct shear test results (tested with Tensar BX4100 at 100 kPa of normal stress and soil compacted to R = 95–96% and aggregate compacted at OMC = 8.2% to R = 94–95%).

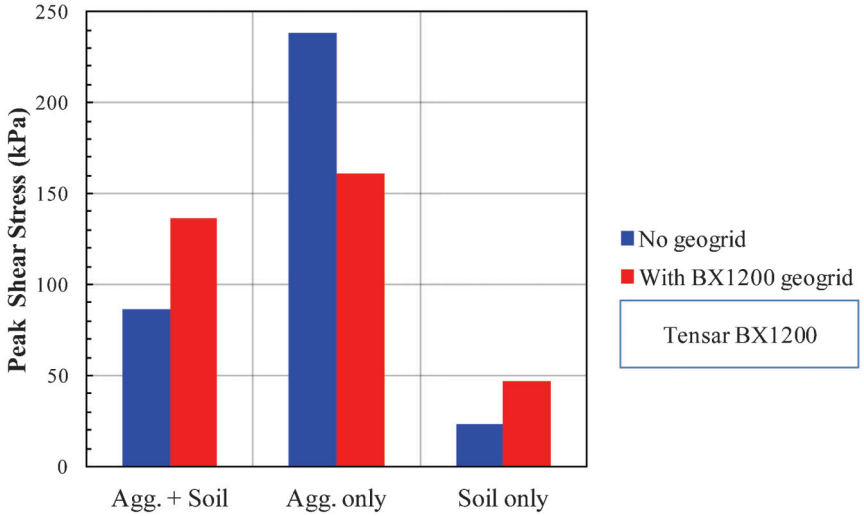

Figure 3.25 Direct shear test results for different materials (tested with Tensar BX1200 with soil compacted at the OMC to relative compaction values of 93–96% (R_{soil} = 94–95% and $R_{aggregate}$ = 93–95%) and a normal stress of 100 kPa).

TABLE 3.11
Peak shear stress and peak interface shear strength coefficient for subgrade soil tested at different moisture contents under a normal stress of 100 kPa

Property	Peak shear stress, τ [kPa] σ_n = 100 kPa		
Moisture content of soil	OMC (%)	OMC + 2%	OMC + 4%
Without geogrid	86.1	69.1	40.0
With geogrid (Tensar BX1200)	136.7	102.6	79.7
Peak interface shear strength coefficient (α_{peak})	1.59	1.49	1.99

Note: Glacial till (CL) soil compacted to R = 95–96% and No. 53 aggregate (GP) compacted at OMC = 8.2% to R = 94%–95%.

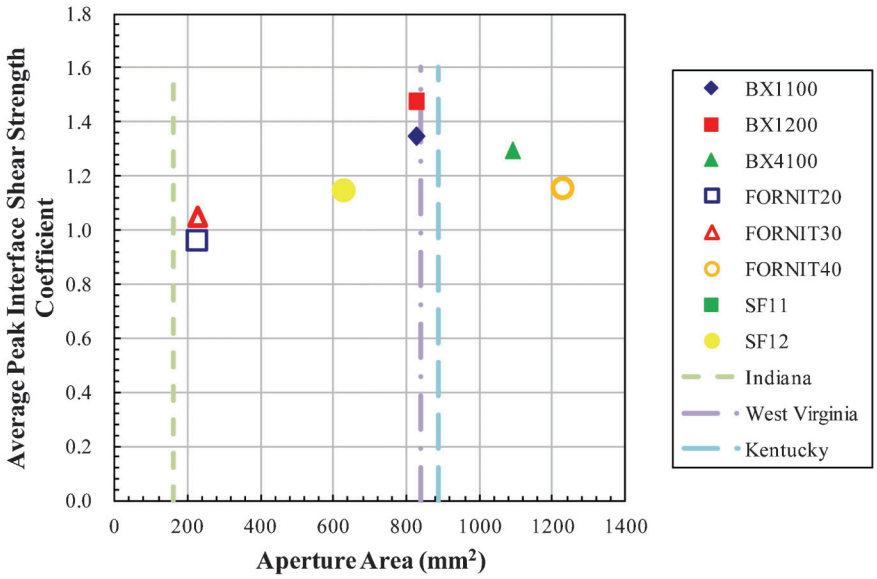

Figure 3.26 Relation between geogrid aperture area, average peak interface shear strength coefficient and property requirements of DOTs' specifications.

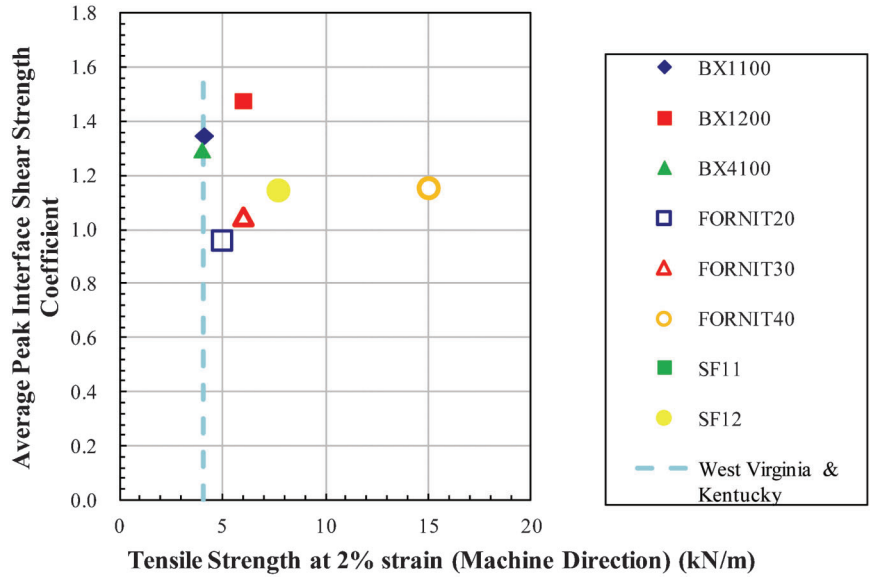

Figure 3.27 Relation between geogrid tensile strength at 2%, average peak interface shear strength coefficient and property requirements of DOTs' specifications.

TABLE 3.12
Peak shear stress and peak interface shear strength coefficient for different test materials tested under a normal stress of 100 kPa

Property	**Peak shear stress, τ [kPa] σ_n = 100 kPa**		
Test material	**Aggregate + soil**	**Aggregate only**	**Soil only**
Without geogrid	86.1	237.9	23.4
With geogrid (Tensar BX1200)	136.7	161.4	47.3
Peak interface shear strength coefficient (α_{peak})	1.59	0.68	2.02

NOTE: Glacial till (CL) soil compacted at OMC = 16.4% to R = 94–95% and No. 53 aggregate (GP) compacted at OMC = 8.2% to R = 93–95%.

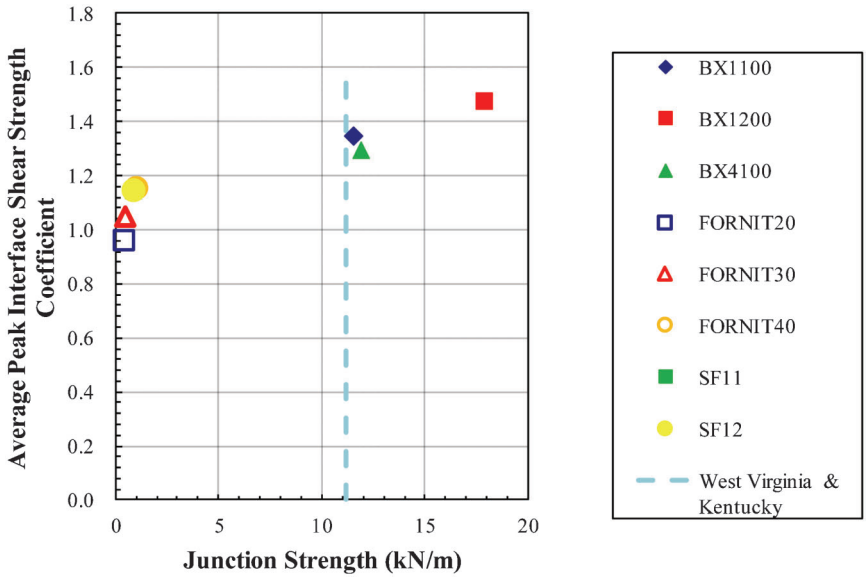

Figure 3.28 Relation between geogrid junction strength (in the machine direction), average peak interface shear strength coefficient and property requirements of DOTs' specifications.

identified in our test results. Currently, INDOT requires a minimum geogrid aperture area of 161 mm^2 (0.25 in^2). Considering the type of aggregates used by INDOT, the current aperture area requirement is not enough to allow an effective development of the reinforcement effect. Accordingly, we suggest that 825 mm^2 (1.28 in^2) of minimum aperture area be required.

Figure 3.27 shows that there is no clear correlation between the tensile strength at 2% strain and the average peak interface shear strength coefficient. In addition, the tensile strength of the tested geogrids satisfy the requirements of all DOTs. The junction strength (in the machine direction) and the efficiency of geogrid reinforcement, as expressed by the average peak interface shear strength coefficient, show a strong correlation (see Figure 3.28). Currently, INDOT does not have any requirement for geogrid junction strength. Thus, a requirement for junction strength needs to be included in INDOT specifications. Figure 3.28 shows that the junction strengths (in the machine direction) of Tensar BX1100, BX1200 and BX4100 geogrids satisfy the junction strength (in the machine direction) requirement (11.2 kN/m = 767 lb/ft) of West Virginia and Kentucky

TABLE 3.13
Material properties of geogrids and geogrid property requirements of DOTs' specifications

	Tensar			HUESKER			Synteen				
Index property	**BX1100**	**BX1200**	**BX4100**	**FORNIT20**	**FORNIT30**	**FORNIT40**	**SF11**	**SF12**	**Indiana DOT**	**West Virginia DOT**	**Kentucky DOT**
Aperture size (mm)	25 33	25 33	33 33	15 15	15 15	15 15	25 25	25 25	12.7 12.7	25.4 33	25.4 34.9
Aperture area (mm^2)	825	825	1089	225	225	225	625	625	161	838	886
Tensile Strength at 2% strain (kN/m)	4.1	6	4	5	6	15	7.7	7.7	—	4.1	4.1
Ultimate tensile strength (kN/m)	12.4	19.2	12.8	13	25	40	34.9	34.9	11.7	8.5	—
Junction strength (kN/m)	11.5	17.9	11.9	0.44	0.47	—	0.87	0.87	—	11.2	11.2
Average peak interface shear strength coefficient (Average α_{peak})	1.35	1.48	1.30	0.96	1.05	1.16	1.15	1.15	—	—	—

TABLE 3.14
Preliminary guidelines for geogrid property requirements

Index property	Unit	Type 1 (biaxial) geogrid	
		Current	Suggested
Aperture size	in (mm)	0.5 (13)	—
	in (mm)	0.5 (13)	—
Aperture area	in^2 (mm^2)	0.25 (169)	1.28 (825)
Junction strength (in the machine direction)	lb/ft (kN/m)	—	788 (11.5)

DOTs. The Tensar BX geogrid provides relatively high efficiency. We suggest that a minimum geogrid junction strength (in the machine direction) value of 11.5 kN/m (788 lb/ft) be required for weak subgrade reinforcement. The proposed preliminary guidelines for subgrade reinforcement are summarized in Table 3.14.

4. CONCLUSIONS

4.1. Summary

The main goal of this study was to evaluate experimentally the mechanical interaction between a subgrade soil and an aggregate base layer, with and without a geogrid at the interface. Eight geogrids were investigated in this study. The peak interface shear strength of soil-soil, soil-aggregate, and aggregate-aggregate without geogrids and with geogrids of various aperture area, junction strength (in the machine direction), and tensile strength was evaluated by performing a series of large-scale direct shear tests. Three different normal stresses (50 kPa, 100 kPa, and 200 kPa) were applied to the top of the samples compacted at the optimum moisture content (OMC_{soil} = 16.4%; $OMC_{aggregate}$ = 8.2%) to relative compaction values of 93–98% (R_{soil} = 94–98%; $R_{aggregate}$ = 93–96%). The effects of the geogrid properties on the performance of the aggregate-geogrid-soil systems were evaluated by comparing the efficiency of different geogrids in terms of the average peak interface shear strength coefficient. Direct shear tests were also performed on samples prepared at moisture contents 2% and 4% higher than the optimum moisture content to assess the effects of different moisture contents of the subgrade soil on the interface shear strength. The effect of geogrid placement on the direct shear box (attached to the upper or lower box) was also examined.

The requirements of geogrid properties in Indiana and other state DOTs' specifications were compared and reviewed. The average peak interface shear strength coefficients obtained from the large direct shear tests were correlated with geogrids properties (aperture area, tensile strength at 2% strain, ultimate tensile strength, and junction strength in the machine direction) and requirements of several DOTs' specifications. Preliminary guidelines for subgrade geogrid reinforcement (aperture area and junction strength) were proposed.

4.2 Conclusions

Based on the findings of the present study, the following conclusions are drawn:

1. The peak shear strength of soil-geogrid-aggregate systems tested at the OMC (OMC_{soil} = 16.4%; $OMC_{aggregate}$ = 8.2%) and compacted to relative compaction values of 93-98% (R_{soil} = 94-98%; $R_{aggregate}$ % 93-96%) under a normal stress of 100 kPa was equal to 114.3 kPa when the Tensar BX4100 geogrid was attached to the lower box and 104.6 kPa when the Tensar BX4100 geogrid was attached to the upper box.
2. The peak shear strength at the interface decreases as the moisture content of the subgrade soil increases. For a normal stress of 100 kPa, the peak interface shear strength coefficient for the subgrade soil sample prepared at the OMC and compacted to relative compaction values of 94-96% (R_{soil} = 95-96%; $R_{aggregate}$ = 94-95%) was 20% less than that of the subgrade soil sample prepared at a moisture content of 4% above the OMC.
3. The large-scale direct shear tests performed on the soil-geogrid-aggregate samples showed that the aperture area and junction strength of the geogrids are important factors affecting the overall interface shear strength. The average values of the three peak interface shear strength coefficients obtained for the three normal stresses (50 kPa, 100 kPa and 200 kPa) considered in this study ranged between 0.96 and 1.48. The peak interface shear strength coefficient depends on the geogrid type, soil and aggregate properties and test conditions. The average peak interface shear strength coefficient increased with increases in the junction strength (in the machine direction) of the geogrid. For the subgrade soil and aggregate considered in this study, the opti-mum aperture area of the geogrid was 825 mm^2 (1.28 in^2). There was no significant correlation between the tensile strength at 2% strain and the average peak interface shear strength coefficient.
4. An aperture area requirement of 825 mm^2 (1.28 in^2) and a junction strength (in the machine direction) requirement of 11.5 kN/m (788 lb/ft) were suggested as preliminary guidelines for weak subgrade geogrid reinforcement based on the results of the large-scale direct shear tests performed in this study and the requirements specified by the DOTs of other states. These recommendations are restricted to the use of geogrid for subgrade reinforcement (Type IV of INDOT specification 207.04) with aggregate No. 53.

REFERENCES

1. INDOT. *2010 Standard and Specifications*. Sections 207 and 918. Indiana Department of Transportation, Indianapolis, 2010.
2. Haas R, J. Wall, and R. G. Carroll. Geogrid Reinforcement of Granular Bases in Flexible Pavements. In *Transportation Research Record: Journal of the Transportation Research Board*, No. 1188, Transportation Research Board of the National Academies, Washington, D.C., 1988, pp. 19–27.
3. Tang, X., G. Chehab, and A. M. Palomino. Evaluation of Geogrids for Stabilizing Weak Pavement Subgrade. *International Journal of Pavement Engineering*, Vol. 9, No. 6, 2008, pp. 413–429.
4. Christopher, B. R., and R. D. Holtz. *Geotextile Engineering Manual*. Report FHWA-TS-86/203. Prepared by STS Consultants Ltd. Northbrook, Illinois, for the Federal Highway Administration, 1985.
5. Giroud, J. P. Geomembrane-Lined Dams in Europe. In *Proceedings of the Geotechnical Fabrics Conference '85*, IFAI, Cincinnati, Ohio, 1985, pp. 66–69.
6. Koerner, R. M. *Designing with Geosynthetics*, 5th ed. Prentice Hall, Upper Saddle River, New Jersey, 1998.
7. Lawson, C. R. Geotextile Revetment Filters. *Geotextiles and Geomembranes*, Vol. 11, Nos. 4–6, 1992, pp. 431–448.
8. Milligan, G. W. E., R. A. Jewell, G. T. Houlsby, and H. J. Burd. A New Approach to the Design of Unpaved Roads–Part I. *Ground Engineering*, Vol. 22, No. 8, 1989, pp. 25–29.
9. Perkins, S. W., and M. Ismeik. A Synthesis and Evaluation of Geosynthetic-Reinforced Base Layers in Flexible Pavements: Part 2. *Geosynthetics International*, Vol. 4, No. 6, 1997, pp. 605–621.
10. Carroll, R. G. Jr., J. C. Wall, and R. Hass. Granular Base Reinforcement of Flexible Pavements Using Geogrids. In *Geosynthetics '87: Conference Proceedings*, New Orleans, February 24–25, 1987, pp. 46–57.
11. Webster, S. L. *Geogrid Reinforced Base Courses for Flexible Pavements for Light Aircraft*. Report No. GL-93-6. Report for the U.S. Department of Transportation/Federal Aviation Administration/Department of Army Geotechnical Laboratory, Vicksburg, Mississippi, 1991.
12. Appea, A. K. In-situ Behavior of Geosynethetically Stabilized Flexible Pavement. M.S, Thesis, Virginia Polytechnic Institute and State University, Blackburg, Virginia, 1997.
13. Berg, R. R., B. R. Christopher, and S. W. Perkins. *Geosynthetic Reinforcement of the Aggregate Base/Subbase Courses of Pavement Structures*. GMA White Paper II. Geosynthetic Materials Association, Roseville, Minnesota, 2000.
14. Houlsby, G. T. and R. A. Jewell. Design of Reinforced Unpaved Roads for Small Rut Depths. In *Proceedings of the 4th International Conference on Geotextiles, Geomembranes and Related Products*, The Hague, Netherlands, Vol. 1, 1990, pp.171–176.
15. Barksdale, R. D., S. F. Brown, and F. Chan. *Potential Benefits of Geosynthetics in Flexible Pavement Systems*. National Cooperative Highway Research Program Report 315. Transportation Research Board of the National Academies, Washington, D.C., 1989.
16. Bell, J. R. Geotextile for Soil Improvement. In *Proceedings of the American Society of Civil Engineers National Convention*, Portland, Oregon, 1980, pp. 1–30.
17. Robnett, Q., and J. Lai. Effects of Fabric Properties on the Performance and Design of Aggregate-Fabric-Soil-Systems. In *Proceedings of the Second International Conference on Geotextiles*, Las Vegas, Vol. 2, 1982, pp. 381–386.
18. De Groat, M., E. Janse, T. A. C. Maagdenberg, and C. Van Den Berg. Design Methods and Guidelines for Geotextile Applications in Road Construction. In *Proceedings of the Third International Conference on Geotextiles*, Vienna, Austria, 1986.
19. Hausmann, M. R. Geotextile for Unpaved Roads- Review of Design Procedures. *Geotextiles and Geomembranes*, Vol. 5, No. 3, 1987, pp. 201–233.
20. Holtz, R. D. and M. E. Harr. *Analytical and Experimental Investigation of Soil Reinforcing*. Report No. ESL-TR-82-31, prepared for Tyndall AFB, Florida. Purdue University, West Lafayette, Indiana, 1983.
21. Al-Qadi, I. L., T. L. Brandon, R. J. Valentine, and T. E. Smith. Laboratory Evaluation of Geosynthetic Reinforced Pavement Sections. In *Transportation Research Record: Journal of the Transportation Research Board*, No. 1439, Transportation Research Board 73rd Annual Meeting, Washington, D.C., 1994, pp. 25–31.
22. ASTM D6637-10. *Standard Test Methods for Determining Tensile Properties of Geogrids by the Single or Multi-Rib Tensile Method*. American Society for Testing and Materials, Philadelphia.
23. Perkins, S. W., M. Ismeik, and M. L. Fogelsong. Mechanical Response of a Geosynthetic-Reinforced Pavement System to Cyclic Loading. In *Proceedings of the Fifth International Conference on the Bearing Capacity of Roads and Airfields*, Trondheim, Norway, Vol. 3, 1998, pp. 1503–1512.
24. Hufenus, R., R. Rueegger, and R. Banjac. Full-Scale Field Tests on Geosynthetic Reinforced Unpaved Roads on Soft Subgrade. *Geotextiles and Geomembranes*, Vol. 24, No. 1, 2006, pp. 21–37.
25. Tang, X., G. Chehab, A. M. Palomino, S. R. Allen, and C. J. Sprague. Laboratory Study on Effects of Geogrids Properties on Subgrade Stabilization of Flexible Pavements. In *Proceedings of GeoCongress 2008*, New Orleans, March 9–12, 2008, p. 310.
26. Juran, I., G. Knochenmus, Y. B. Acar, and A. Arman. Pull-out Response of Geotextiles and Geogrids (Synthesis of Available Experimental Data). In *Geosynthetics for Soil Improvement*, Holtz, R.D., Ed. Geotechnical Special Publication No. 18, ASCE, proceedings of symposium held in Nashville, Tennessee, 1988, pp. 92–111.
27. Cancelli, A., P. Rimoldi, and S. Togni. Frictional Characteristics of Geogrids by Means of Direct Shear and Pullout Tests. In *Proceedings of the International Symposium on Earth Reinforcement Practice*, Kyushu Univ., Fukuoka, Japan, 1992, pp. 51–56.
28. Cazzuffi, D., L. Picarelli, A. Ricciuti, and P. Rimold. Laboratory Investigations on the Shear Strength of Geogrid Reinforced Soils. *ASTM Spec. Tech. Publ.*, No. 1190, 1993, pp. 119–137.
29. Liu, C. N., J. G. Zornberg, T. Chen, Y. Ho, and B. Lin. Behavior of Geogrid-Sand Interface in Direct Shear Mode. *Journal of Geotechnical and Geoenvironmental Engineering*, Vol. 135, No. 12, 2009, pp. 1863–1871.
30. GMA. *Geosynthetics in Pavement Systems Applications: Section One: Geogrids, Section Two: Geotextiles*. Prepared for AASHTO. Geosynthetics Materials Association, Roseville, Minnesota, 1999.
31. ASTM D4595-05. *Standard test methods for Determining Tensile Properties of Geotextiles by the Wide-Width Strip*

Method. American Society for Testing and Materials, Philadelphia.
32. U.S. Army Corps of Engineers. *CW-02215 Determination of Percent Open Area*.
33. ASTM D4355-05. *Standard test methods for Deterioration of Geotextiles by Exposure to Light, Moisture and Heat in Xenon Arc Type Apparatus*. American Society for Testing and Materials, Philadelphia.
34. ASTM D5362. *Standard Test Method for Snagging Resistance of Fabrics (Bean Bag)*. American Society for Testing and Materials, Philadelphia.
35. GRI. *GRI Test Methods & Standards*. Geosynthetic Research Institute, Drexel University, Philadelphia, 1998.
36. Rainey, T., R. D. Barksdale, and R. Schmertmann. Construction Induced Reduction in the Tensile Strength of Polymer Geogrids. In *Proceedings, Geosynthetics '93: Conference Proceedings*, Vancouver, B.C., March 30–April 1, 1993.
37. Kansas Department of Transportation. *Special Provision to the Standard and Specification*, Section 1710, 2007.
38. State of Ohio Department of Transportation. *Geogrid for Subgrade Stabilization*. Supplemental Specification, Section 861, 2010.
39. West Virginia Division of Highways. *Standard Specifications Roads and Bridges*. Division 200 and Section 206, 2010.
40. Kentucky Department of Transportation. *Standard and Specification*, Section 843, 2004.
41. ASTM D5321-08. *Standard Test Methods for Determining the Coefficient of Soil and Geosynthetic or Geosynthetic and Geosynthetic Friction by the Direct Shear Method*, American Society for Testing and Materials, Philadelphia.
42. ASTM D2487. *Standard test methods for Classification of Soils for Engineering Purposes (Unified Soil Classification System)*. American Society for Testing and Materials, Philadelphia.
43. AASHTO M 145-91. *Classification of Soils and Soil-Aggregate Mixtures for Highway Construction Purposes*. AASHTO DESIGNATION, American Association of State Highway and Transportation Officials, Washington, D.C., 1993, pp. 122–126.
44. ASTM D4318. *Standard Test Methods for Liquid Limit, Plastic Limit, and Plasticity Index of Soils*. American Society for Testing and Materials, Philadelphia.
45. ASTM D422-63. *Standard Test Method for Particle-Size Analysis of Soils*. American Society for Testing and Materials, Philadelphia.
46. ASTM D698. *Standard Test Methods for Laboratory Compaction Characteristics of Soil using Standard Effort*. American Society for Testing and Materials, Philadelphia.